Chapter 2

Constitutive relationship of Magnetostrictive Materials

2.1 Introduction

Constitutive relationship of magnetostrictive materials consists of a sensing and an actuation equation. In sensing equation magnetic flux density is a function of applied magnetic field and stress, and in actuation equation, strain is function of applied magnetic field and stress. Both sensing and actuation equations are coupled through magneto-mechanical coupling coefficient. Hence, to obtain the correct constitutive law of this material, both equations need to be solved simultaneously. This chapter gives the complete details of the numerical characterization of constitutive relations of magnetostrictive material such as Terfenol-D.

2.1.1 Existing Literature

Existing literature in this particular area is limited. However, there are some works that are very relevant, which is used in this chapter for the constitutive model development. Anjanappa and Wu [17] developed a mathematical model for a magnetostrictive particulate actuator based on the magnetoelastic material property. Ackerman et al. [3] developed an analytical approach for formulation of input-output representations for magnetostrictive actuators through the application of an impedance modelling method, which included the mechanical dynamics and the electro-magneto-mechanical interaction of the actuator device. Anhysteretic nonlinear constitutive relationships was studied by Krishna Murty et al. [192], where the magnetostriction was considered as fourth order polynomial of applied magnetic field for different stress level. Dapino et al. [95] modelled the strains and forces generated by magnetostrictive transducers considering both

the rotation of magnetic moments and the elastic vibrations in the transducer. Wakiwaka et al. [384] studied the effect of the magnetic bias for which largest linear range was available depending on each pre-stress level. Kannan and Dasgupta [174] developed quasi-static Galerkin finite-element theory for modelling magneto-mechanical interactions at the macroscopic level considering body forces and coupled constitutive nonlinearities. Kondo [190] examined the dynamic behavior of giant magnetostrictive materials.

2.1.1.1 Coupling between Actuation and Sensing Equations

Analysis of smart structures using magnetostrictive materials are generally performed using uncoupled models. Uncoupled models are based on the assumption that the magnetic field within the magnetostrictive material is proportional to the electric coil current times the number of coil turn per unit length (coil constant). Due to this assumption, actuation and sensing equations gets uncoupled. For an actuator, the strain due to magnetic field (which is proportional to coil current) is incorporated as the equivalent nodal load in the finite element model for calculating the block force. Thus, with this procedure, analysis is carried out without taking smart degrees of freedom in the finite element model. Similarly for a sensor, where generally coil current is assumed zero, the magnetic flux density is proportional to mechanical stress, which can be calculated from the finite element results through post-processing. This assumption on magnetic field, leads to the violation of flux line continuity, which is one of the four Maxwell's equations in electromagnetism. To satisfy Maxwell equation of flux conservation and the associated constitutive relationships, the magnetic field should become a function of mechanical condition of the material and this is called coupled formulation.

The constitutive model for a magnetostrictive material is essentially a coupled one. That is, the strains and magnetic flux density are developed due to both mechanical stress and magnetic field intensity. In coupled model, it is considered that magnetic flux density and/or strain of the material are functions of stress and magnetic field, without any additional assumption on magnetic field, unlike the uncoupled model. Benbouzid et al. modelled the static [34] and dynamic [36] behavior of the nonlinear magneto-elastic medium for magneto-static case using finite element method. Magneto-mechanical coupling was incorporated considering both permeability and elastic modulus as functions of stress and magnetic field. However, all these works do not provide a convenient way for analysis of magnetostrictive smart structure, when the coupling feature is considered. In this chapter, coupled features of magnetostrictive materials are used in a finite element

formulation, which has both magnetic and mechanical degrees as unknown degrees of freedom. In addition, it is shown that the magnetic field is not proportional of applied coil current (which is the assumption of the uncoupled model), and it depends on the mechanical stress on the magnetostrictive material. This chapter also shows that the coupled model preserve the flux line continuity, which is one of the drawback of uncoupled model.

2.1.1.2 Nonlinearity of Magnetostrictive Materials

The constitutive relations of magnetostrictive materials are essentially nonlinear [52]. The prediction of behavior of magnetostrictive material, in general, is extremely complicated due to its hysteretic non-linear character. In structural application, due to these nonlinear material properties, modelling of the system will also become nonlinear. Hence to model the exact nonlinear behavior of the structure, modelling of these nonlinear properties of magnetostrictive materials is essential.

Magnetostriction, which is the strain due to magnetic field, is a nonlinear function of applied magnetic field. At low value of magnetic field, the slope of the curve is low, while at medium value of magnetic field, the slope is high and again at high magnetic field levels, the slope becomes low [52]. In addition, these magnetic field-magnetostriction curves are different for different compressive stress level. Hence, nonlinear modelling of magnetostriction in terms of prestress level and applied magnetic field is a difficult task. However, the nonlinear representation of permeability in terms of magnetic field and stress level is addressable. Also, the strain always remains positive for either positive or negative applied field for positive magnetostriction. Therefore, the vibration frequency will be twice that of the magnetic field if the magnetostrictive material is subjected to an alternating current. This is the so-called double frequency effect. However, this double frequency effect in actuation equation is generally bypassed using bias current to keep the coil current always positive.

Traditionally, the nonlinear behavior of magnetostrictive material is studied using uncoupled model. In uncoupled model, nonlinear actuation and sensing properties are examined separately. For actuation, the magnetostriction for different stress level at a particular applied magnetic field is studied. Similarly, for sensing application, the generated magnetic flux density for different applied stress levels, are studied. Earlier study to model uncoupled nonlinear actuation of magnetostrictive material was done in reference [192] by considering a fourth order polynomial of magnetic field for each stress

level. In this approach, stress level for which curve is not available, the coefficients of the curve will have to be interpolated from the coefficients of nearest upper and lower stress level curves. Similar approach is used in this chapter to study the nonlinear behavior of both coupled and uncoupled formulation. In this chapter, this nonlinear representation is modelled using different techniques such as, polynomial curve fitting and artificial neural network.

2.1.1.3 Hysteresis of Magnetostrictive Materials

Hysteresis behavior of magnetic material can be described by a curve having three parts. First part represents the linear material behavior, the second part represents non-linear material behavior including saturation, and the third part describes hysteresis effects like remanence, coercivity, static losses and accommodation. The first analytic model of ferromagnetic hysteresis was proposed by Rayleigh [323]. Adly, and Hafiz, [7] constructed and identified hysteresis of magnetostriction using Preisach-type model through experimental training data to a modular discrete Hopfield neural network–linear neural network combination. Calkins, et al. [53] addresses the modelling of hysteresis in magnetostrictive transducers based on the Jiles-Atherton mean field model for ferromagnetic hysteresis in combination with a quadratic moment rotation model for magnetostriction. Adly, et al. [11] presented an approach for simulating 1-D magnetostriction using 2-D anisotropic Preisach-type models, where measured flux density versus field and strain versus field curves for different stress values was taken into account for identification of the model. Adly, and Hafiz, [8] proposed that artificial neural network be used as a tool to accomplish the identification task of classical Preisach model, where the congruency property is not exactly valid and hence required more appropriate experimental data during the identification stage to improve the model accuracy. Adly, and Mayergoyz, [9] presented anisotropic vector Preisach-type hysteresis models of magnetostrictive material for simulating field-stress effects on magnetic materials. Adly, et al. [10] suggested an identification process of two-dimensional Preisach model for modelling of one-dimensional magnetostriction using neural network. Debruyne, et al. [96] proposed a method to characterize the Preisach model of hysteresis phenomenon of magnetic material by taking a normal distribution law for the switching field density. Benabou, et al. [33] presented and implemented in a finite element code, Preisach and the Jiles-Atherton (J-A) models of hysteresis and compared these models in terms of accuracy, numerical implementation and computational effort. Yu, et al. [417] presented the rate-dependent hysteresis property by introducing the de-

pendence of the Preisach function on the input variation rate to adjust the relationship of hysteresis loop on the input variation rate for different hysteresis systems. Cheng, et al. [76] proposed a dynamic model which considers the eddy current, hysteresis and anomalous losses based on Preisach modelling. Ktena, et al. [193] used a least-squares parameter fitting procedure for one-dimensional (1D) and two-dimensional (2D) formulations of the Preisach hysteresis in ferromagnets, and shape memory alloys. Ktena, et al. [194] identified hysteresis using data from a major hysteresis curve and a least-squares error minimization procedure for the parameters of the characteristic density. Dupre, et al. [112] modelled the hysteresis of material like the SiFe-alloys using the Preisach theory, took the magnetization as input to the model. Natale, et al. [288] proposed the identification and compensation of the hysteretic behavior of Terfenol-D actuator by applying the classical Preisach model, whose identification procedure is performed by adopting of both a fuzzy approximator and a feed-forward neural network. Ragusa [318] presented an analytical computation of the factorized distribution function by moving Preisach model starting from a set of measured symmetrical loops. A probabilistic model for magnetostrictive and magnetic hysteresis in Terfenol-D compounds is proposed by Armstrong [24]. The critical stresses that eliminate hysteresis in magnetostrictive materials were determined by Cullen et al. [93] for coherent magnetization reversal. From these works, it can be concluded that the prediction of behavior of magnetostrictive material, in general, is extremely complicated due to its hysteretic non-linear character.

The main goal of this chapter is to numerically characterize the constitutive model of the magnetostrictive material for its use in structural health monitoring applications. One of the main issues in the design of these magnetostrictive sensors/actuators is to predict its behavior under various mechanical and/or magnetic excitation conditions through the constitutive relationship of material. Anhysteretic sensing and actuation properties of magnetostrictive materials (Terfenol-D) are taken into consideration in the structural analysis for singled valued sensing and actuation. Hence only anhysteretic models of magnetostrictive material are studied in this chapter.

The chapter is organized as follows. In Section-2.2, uncoupled formulation is developed for magnetostrictive materials. The anhysteretic modelling of magnetostrictive material for linear-uncoupled and nonlinear-uncoupled constitutive relationships is given. Subsequently, coupled formulations for both linear and nonlinear are given in Section-2.3 for magnetostrictive materials. For both linear and nonlinear models, total mechanical and magnetic energy is calculated for a magnetostrictive rod. Hamiltonian principle is

used to get the equations for magnetic and mechanical degrees of freedoms. Nonlinear modelling of magnetostrictive material is studied with polynomial approach as well as ANN approach. Finally, the findings of this chapter are summarized in Section-2.4.

2.2 Uncoupled Constitutive Model

Application of magnetic field causes strain in the magnetostrictive material (Terfenol-D) and hence the stress, which changes magnetization of the material. As described by Butler [52], Moffett et al [273], and Hall and Flatau [142], the three-dimensional linear coupling constitutive relationship between magnetic and mechanical quantities for magnetostrictive material are given by

$$\{\epsilon\} = [S^{(H)}]\{\sigma\} + [d]^T\{H\} \tag{2.1}$$

$$\{B\} = [\mu^{(\sigma)}]\{H\} + [d]\{\sigma\} \tag{2.2}$$

where $\{\epsilon\}$ and $\{\sigma\}$ are strain and stress respectively. $[\mathbf{S^{(H)}}]$ represents elastic compliance measured at constant $\{\mathbf{H}\}$ and $[\mu^{(\sigma)}]$ represents the permeability measured at constant stress $\{\sigma\}$. Here $[\mathbf{d}]$ is the magneto-mechanical coupling coefficient, which provides a measure of the coupling between the mechanical strain and magnetic field. In general, $[\mathbf{S}]$, $[\mathbf{d}]$ and $[\mu^{\sigma}]$ are nonlinear as they depend upon $\{\sigma\}$ and $\{\mathbf{H}\}$. However, reasonable response estimation can be obtained by treating them as linear [52].

Equation-(2.2) is often referred to as the converse effect and Equation-(2.1) is known as the direct effect. These equations are traditionally used for sensing and actuation purpose. It should be noted that the elastic constants used correspond to the fixed magnetic field values and the permeability correspond the fixed stress values. Here we propose to use an ANN model to characterize the constitutive model and compare the solution with the reference [192].

Here the experimental data for training of ANN, is taken from Etrema manual [52] for Terfenol-D, a giant magnetostrictive material. Experimental data given in the manual for two different set of curves, namely the of magnetostriction - magnetic field variation for different stress level is shown in Figure-2.1 and Figure-2.2, and the stress - strain curves for different magnetic field levels is shown in Figure-2.3 and Figure-2.4. Here uncoupled constitutive relationship of magnetostrictive material is considered for the study. Analysis of smart structures using magnetostrictive materials as either sensors or actuators has traditionally been performed using uncoupled models. Uncoupled models make the assumption that the magnetic field within the magnetostrictive material is constant and

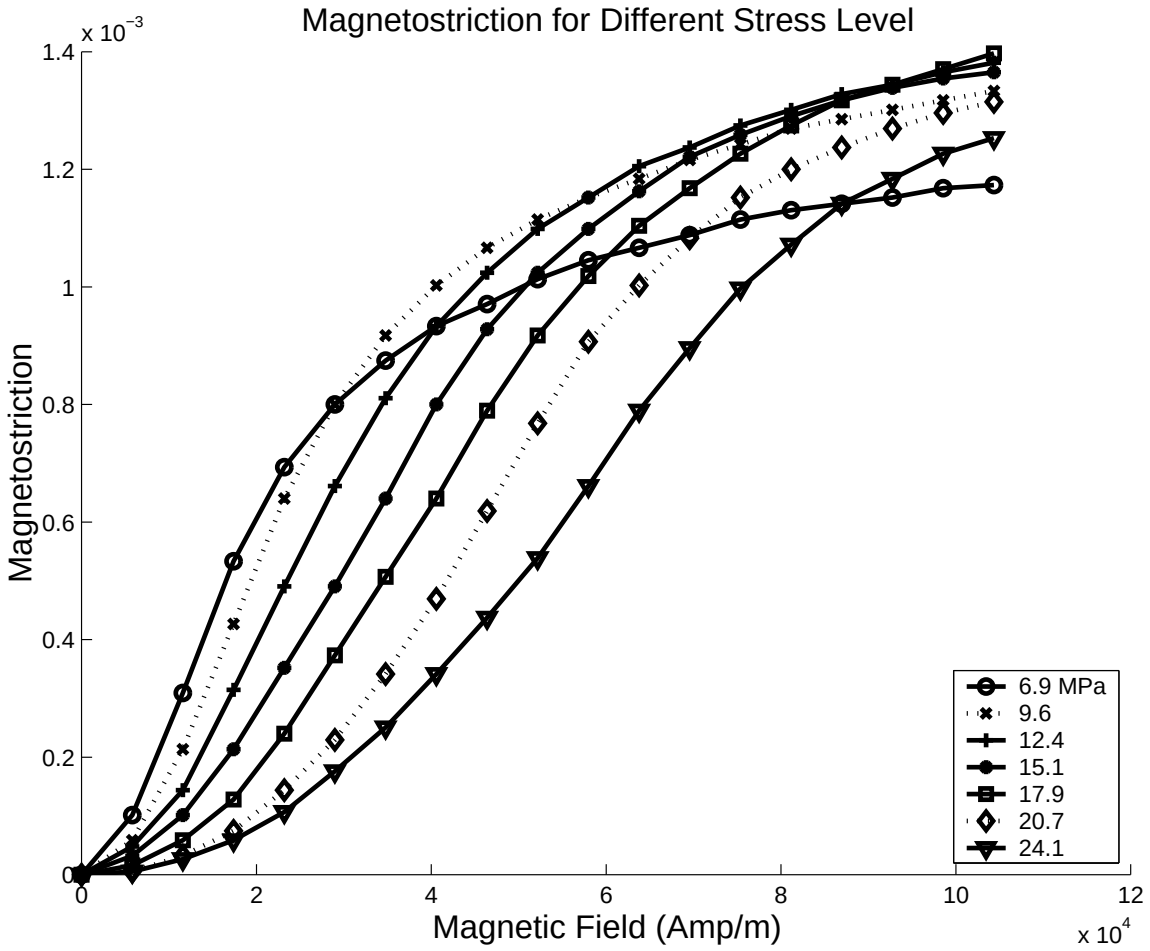

Figure 2.1: Magnetostriction vs. magnetic field supplied by Etrema

proportional to the product of electric coil current and the number of coil turn per unit length. Magnetostriction $\lambda = [d]^T\{H\}$ is the strain due to magnetic field, which is the second term in the Equation-(2.1). Hence, the strain induced by an actuator and the magnetic flux density output of a sensor, are described by two uncoupled equation. This makes analysis of a smart structure relatively simpler. For this uncoupled model, both linear and nonlinear analysis is performed. In the linear model, the magnetomechanical-coupling term is assumed as constant. But generally it is a nonlinear function of magnetic field and stress level. In the nonlinear model, the magnetostriction is modelled with a three layer artificial neural network as it can approximate any nonlinear input-output relationships through its universal approximation theorem [150].

From experimental data [52], only longitudinal component of magnetostriction due

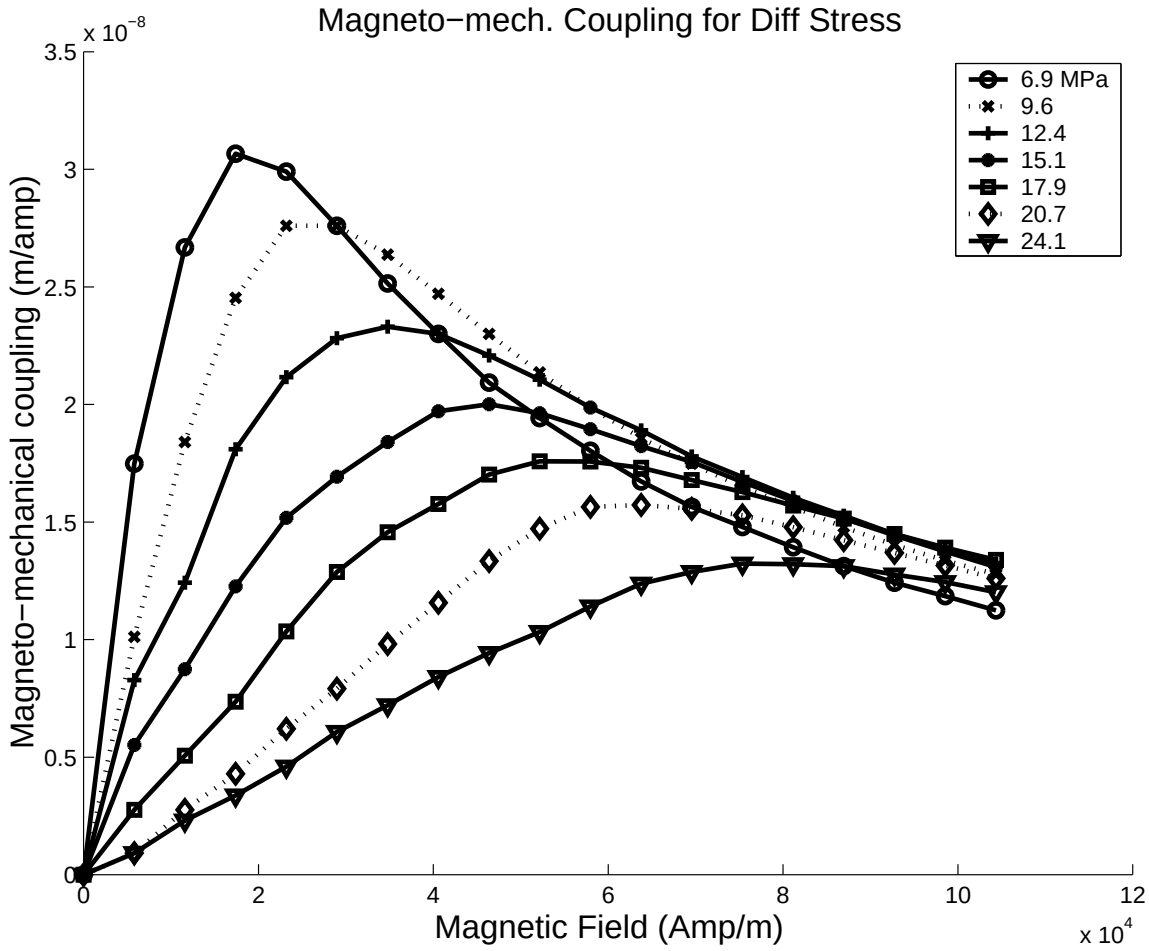

Figure 2.2: Magneto-mechanical coupling vs. magnetic field supplied by Etrema

to longitudinally applied magnetic field is present, and hence only d_{33} component is available. Magnetostriction in this experiment is $d_{33}H_3$. All other component of $[\mathbf{d}]$ matrix is considered equal to zero. In the absence of sensing experimental data, where an application of magnetic field and stress will produce magnetic flux form magnetostrictive sensor (due it its inverse magnetostrictive effect, Villery Effect), sensing equation is not studied here. In addition, actuation data for tensile stress level is also not available in the manual.

2.2.1 Linear Uncoupled Model

Although magnetostriction is highly nonlinear with magnetic field and stress, sometimes the linear actuation model is quite sufficient especially in vibration and noise control application. To get the linear actuation from this highly nonlinear property, some magnetic

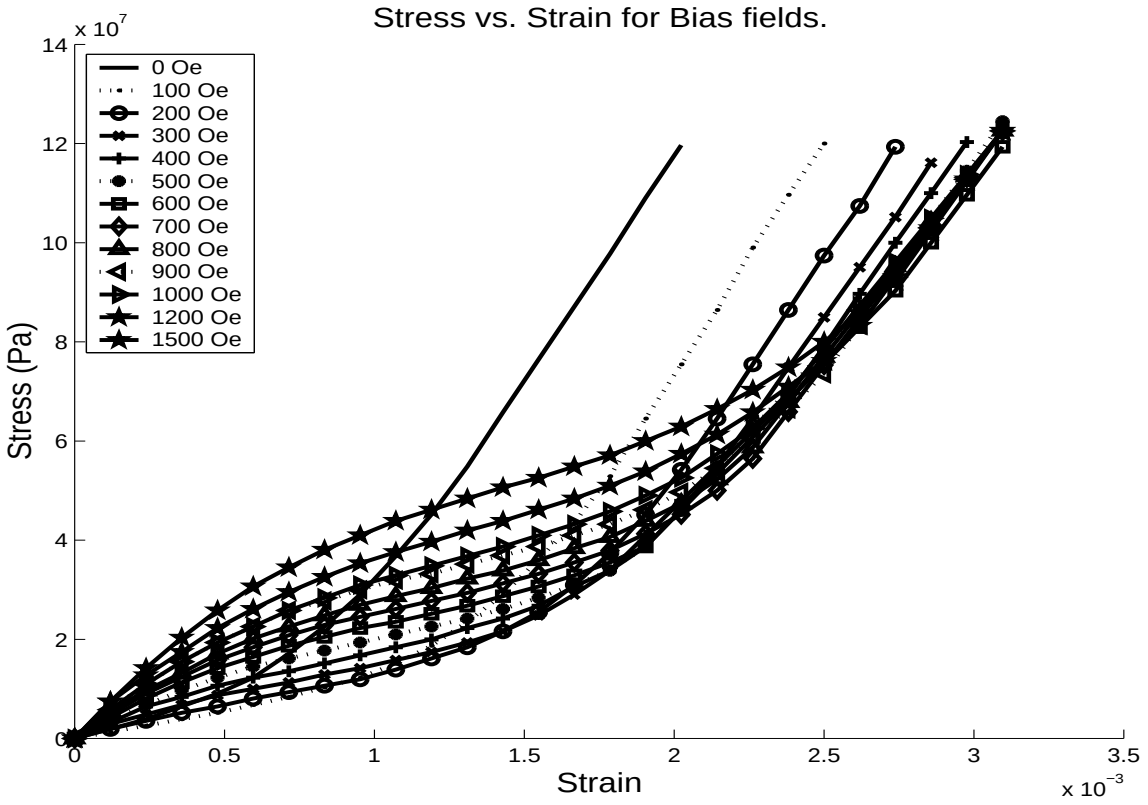

Figure 2.3: Stress vs. strain relationship for different magnetic field level [Etrema]

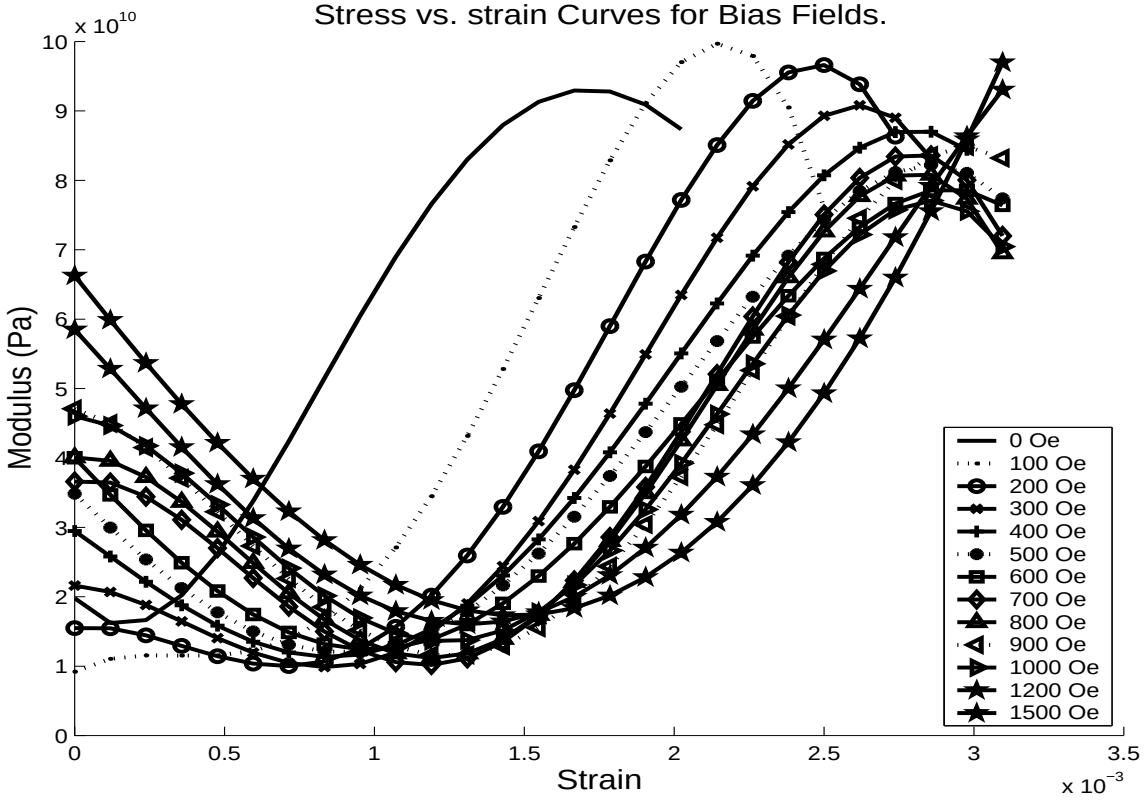

Figure 2.4: Elasticity vs. strain relationship for different magnetic field level [Etrema]

and mechanical bias is used, which will shift the starting point of curves in the middle of linear range. Hence, there is a necessity for calculation of optimum values of bias magnetic field and bias stress to give maximum linear range of actuation and maximum value of tangential coupling coefficient [384]. This is a multi objective optimization problem where maximum range of linearity as well as tangential coupling coefficient is required. In addition, minimization of bias magnetic field and bias stress level may be other design criteria. If permanent magnets are used for bias magnetic field, energy requirement for constant DC current will not be required.

2.2.1.1 Actuator Design - Some Issues

It is described that the designed actuator are required to satisfy the following two consideration; one, it has to behave as linear as possible, and the second; it should be efficient. The issues relating to these two criteria are discussed below.

2.2.1.2 Linearity

Figure-2.5 and Figure-2.6 give the variation of tangential coupling and coupling coefficient with the bias field obtained by polynomial fitting of experimental data [52], and it is shown that for 15.1 MPa bias stress level, the linear range of actuator is from 0 to 40kA/m with tangential coupling value 2e-8 m/amp, and for 24.1 MPa bias stress linear range is from 50 to 70kAmp/m with tangential coupling value 1.8e-8 m/Amp. Hence, 15.1 MPa stress bias with 30 kA/m bias magnetic field is the optimal value for having higher tangential coupling. But in general for any application, the stress level of actuator will not be constant and hence this study will not be effective if the stress level changes.

2.2.1.3 Efficiency

The efficiency of actuator is defined as the ratio of mechanical energy to the magnetic energy. Hence, the increased value of magneto-mechanical coupling coefficient will increase the efficiency of actuator. Considering bias magnetic field will be obtained by a permanent magnet, the optimum bias magnet required for higher efficiency of actuator will simply be equal to the average magneto-mechanical coupling coefficient. The optimum value of bias magnetic field for the average magneto-mechanical coupling coefficient is given in Figure-2.6. Here, the average magneto-mechanical coupling coefficient is calculated for different stress level and different bias magnetic field. It is shown that for low stressed actuator, low strength bias magnet is optimum, while as for high stressed actuator, high strength

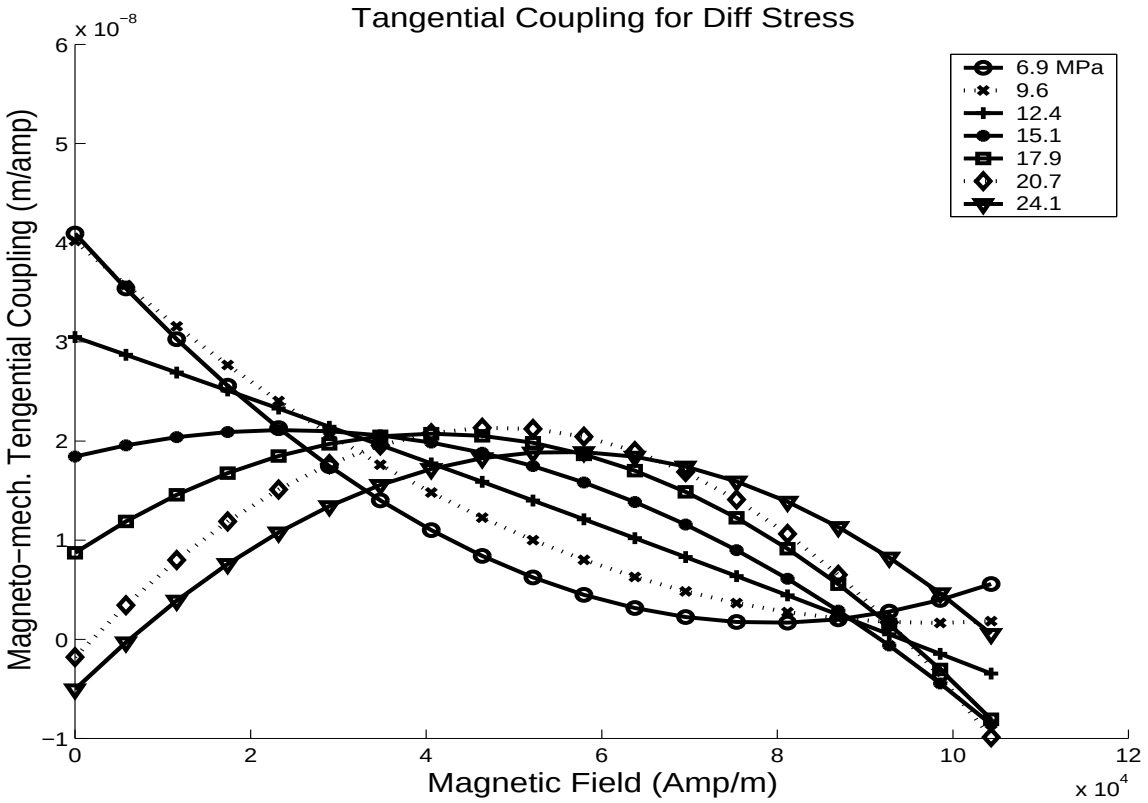

Figure 2.5: Tangential coupling with bias field for different stress level.

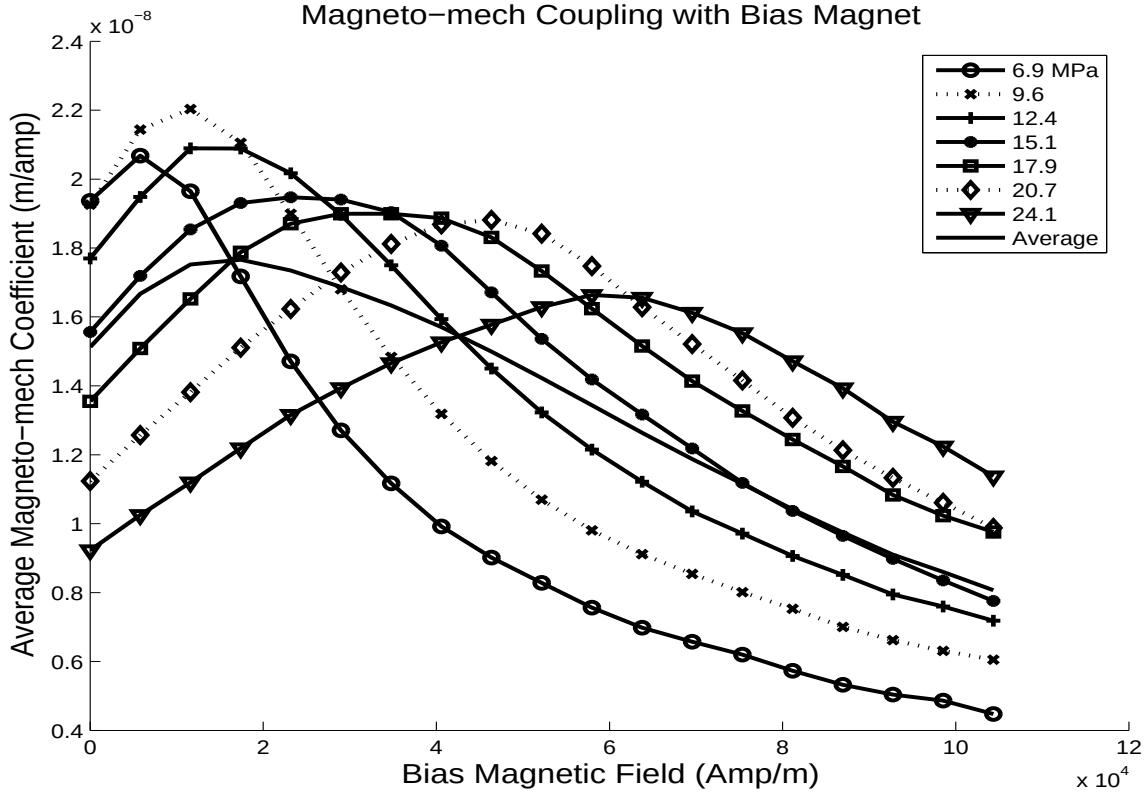

Figure 2.6: Coupling coefficient with bias field for different stress level.

bias magnet is optimum for increased value of average coupling coefficient. These average values for different stress level is again averaged over the stress level and shown that the strength of 20-kA/m bias magnet is optimum for efficiency of magnetostrictive actuator in varied stress level. Average magnetomechanical coefficient with zero magnetic bias is 14.67e-9 (m/amp) (shown in Figure-2.6). This value is generally considered in uncoupled, linear, bias-less magnetostrictive actuator. From Figure-2.1, it is clear that the linear model is an approximation from the real behavior of the actuator.

2.2.2 Polynomial Approach

In the polynomial approach [192], every magnetostriction-magnetic field intensity curve is represented by a fourth order polynomial curve given by.

$$\lambda = \alpha_0 + \alpha_1 H + \alpha_2 H^2 + \alpha_3 H^3 + \alpha_4 H^4 \tag{2.3}$$

Where, λ represent the magnetostriction and, H is the applied magnetic field. The constants $\alpha_0 - \alpha_4$ are evaluated for each stress level using the data supplied by Etrema manual, and their values are listed in Table-2.1. A linear interpolation of functional form for these constants $\alpha_1 - \alpha_4$ is estimated as a function of σ, which is used whenever integration with σ is required in this analysis. This is given by

$$\begin{aligned} \alpha_i &= \alpha_{i1} \qquad \sigma < \sigma_1 \\ \alpha_{ij}(\sigma) &= \alpha_{ij} + \frac{\alpha_{i(j+1)} - \alpha_{ij}}{\sigma_{j+1} - \sigma_j}(\sigma - \sigma_j) \qquad \sigma_j < \sigma < \sigma_{j+1} \\ & i = 0, 1, 2, 3, 4 \qquad j = 1, 2, 3, 4, ...6 \end{aligned} \tag{2.4}$$

The values of α_{ij}'s and σ_j's are given in Table-2.1. The magnetomechanical constant

Table 2.1: Constants α_0 through α_4 for different prestress levels [192].

σ_j, MPa	6.9	9.6	12.4	17.9	24.1	38.0
α_{0j}	-50.2987	-81.3171	-58.7017	-2.1391	22.0131	-0.4968
α_{1j}	3.7301	3.2017	1.9530	-0.0931	-0.5268	0.2066
α_{2j}	-4.7e-3	-2.3e-3	9.72e-4	5.1e-3	3.6e-3	-3.7006e-4
α_{3j}	2.8406e-6	4.0316e-7	-2.4375e-6	-5.2425e-6	-2.5378e-6	1.3335e-6
α_{4j}	-6.4174e-10	1.1572e-10	9.095e-10	1.5458e-9	4.9722e-10	-5.7574e-10

now can be expressed by differentiating Equation-(2.3). This is given by

$$d = \alpha_1 + 2\alpha_2 H + 3\alpha_3 H^2 + 4\alpha_4 H^3 \tag{2.5}$$

2.2.3 ANN Model

As mentioned earlier, magnetostriction varies with of applied magnetic field and stress level. In this study, the magnetostriction is modelled using a three layer artificial neural network (ANN) trained by back propagation algorithm for compressive stress level. In input layer, two input nodes are used; one for applied magnetic field and other for stress level and in output layer, one output node for magnetostriction is used. This artificial neural network is trained using the experimental data given in Etrema manual [52] for different compressive stress level. Due to non-availability of experimental data in tensile stress level, magnetostriction for tensile stress level is not modelled here. As magnetostriction depends upon stress level and applied magnetic field, using trained neural network, the corresponding magnetostriction ($d_{33}H_3$) is calculated for applied magnetic field and stress level.

2.2.3.1 Network Architecture

The network parameters are determined, as is common practice, through trial and error. This includes the number of layers, the number of nodes in hidden layers and the learning rates. Number of hidden layers is assumed as one to simplify the study and reduce the size of network architecture. Hence, the network used consisted of three layers: one input layer of two neurons (one for each input variable, stress and magnetic field), one hidden layer of different no of neurons (nodes) and one output layer of one neuron, which in the present case represents magnetostriction. A study for the performance of network is done to determine the effect of number of nodes in the hidden layer. Similarly, the effect of learning rate and learning algorithm is also studied.

2.2.3.2 Study on Number of Nodes in Hidden Layer

Although the increasing number of hidden layer nodes will represent the actuation nonlinearity more accurately, the floating point operation and storage requirement for the evaluation of magnetostriction for different stress levels and applied magnetic fields using the trained architecture will also increase. Hence, there will be a tradeoff between the number of nodes in hidden layer and performance of trained network from the training and validation samples. Performance of the network can be assessed if one can measure the error associated with the learning performance and the strains for different number of nodes in the hidden layer. These are plotted in Figure-2.7 and Figure-2.8. From the

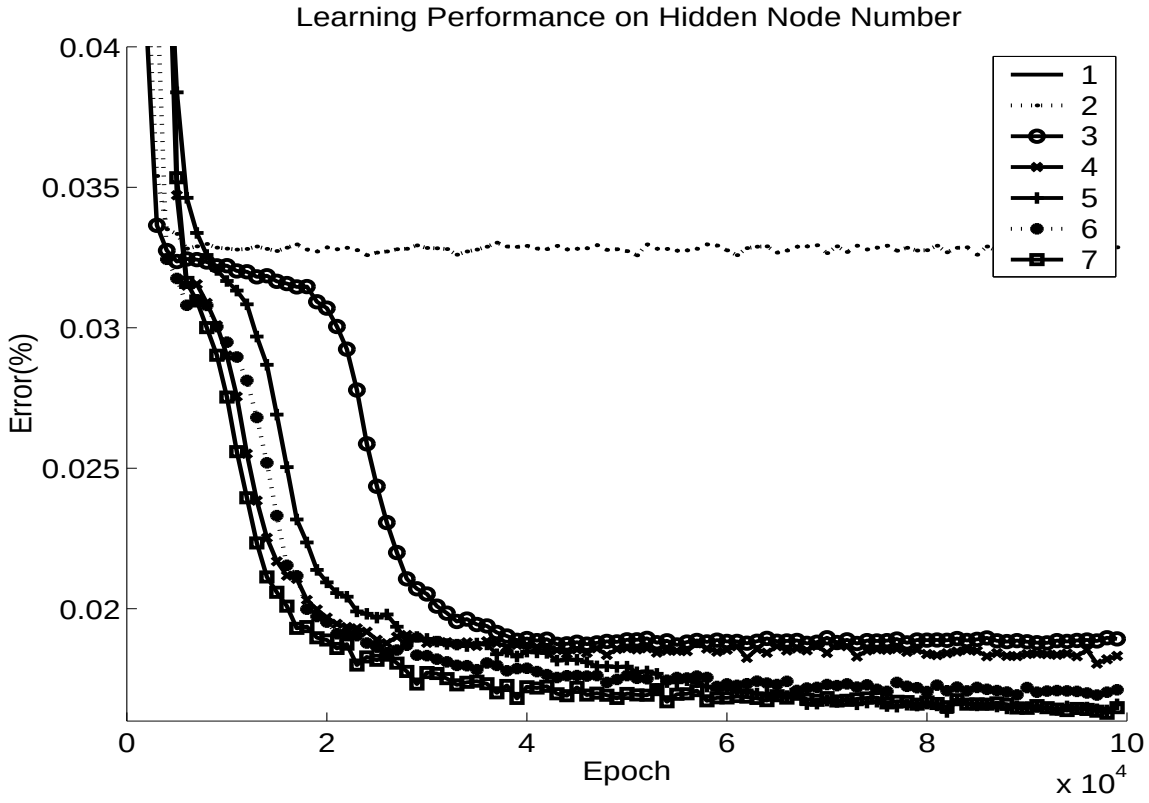

Figure 2.7: Study on the effect of number of node in hidden layer.

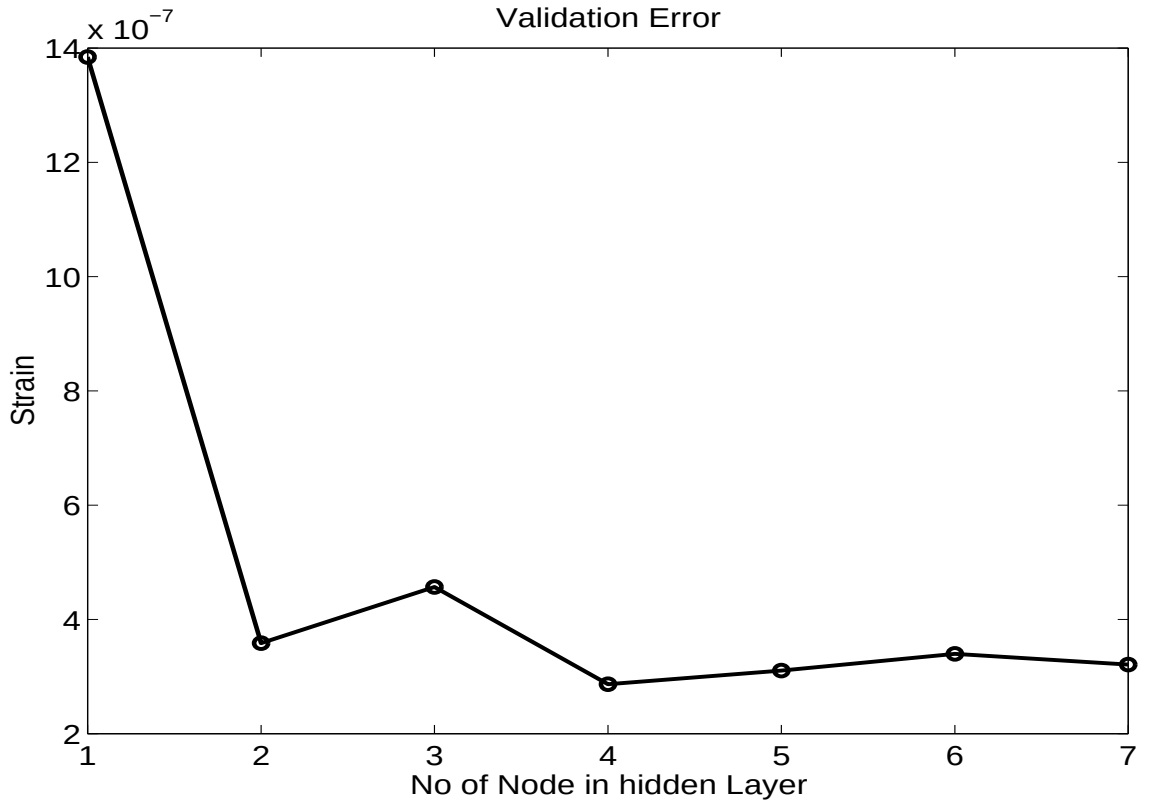

Figure 2.8: Study on the effect of number of node in hidden layer.

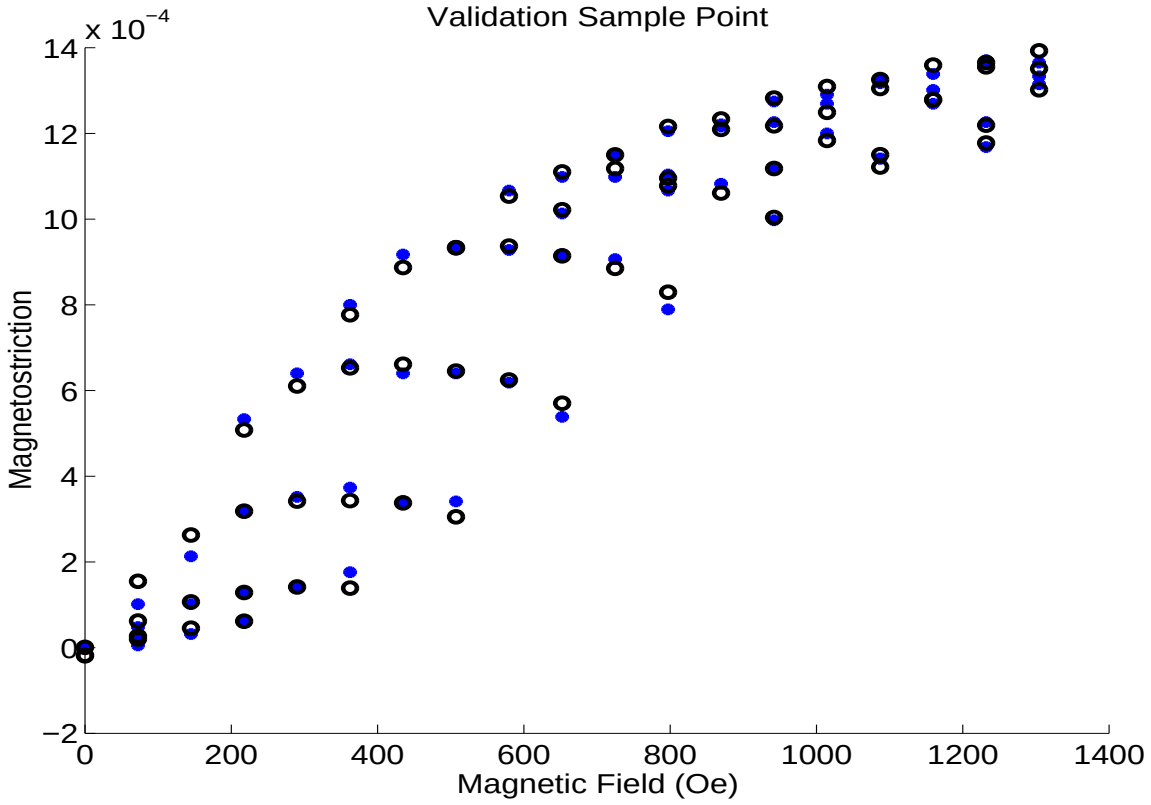

Figure 2.9: Test data from network and sample data set.

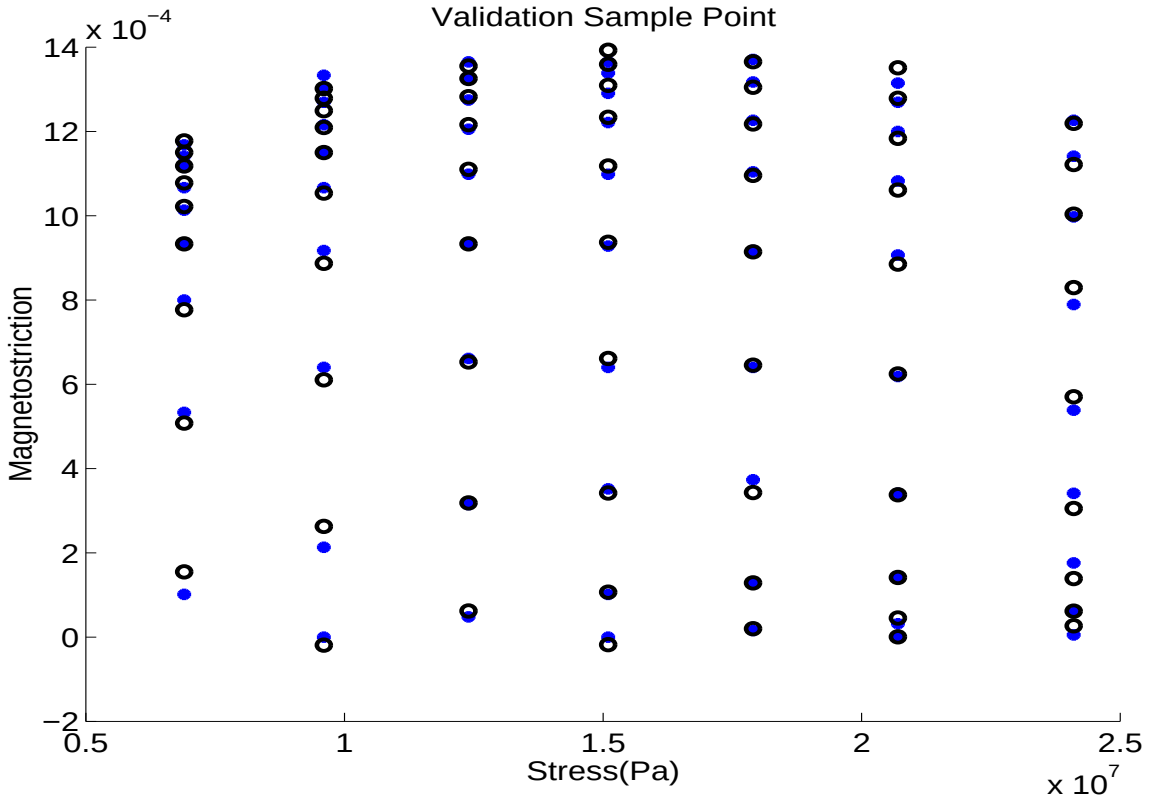

Figure 2.10: Test data from network and sample data set.

figure, it is found 4-nodded network is optimum. Except 1 and 2-nodded network, training performance of other networks are comparatively acceptable. But for 3-nodded and 5-nodded architectures, the validation errors are poor compared to 4-nodded architecture. Average error of validation samples in 4-nodded architecture is around 0.2 micro-strain. Hence, 4-nodded architecture is considered for further study. Test data is plotted in two different projection planes one in stress vs. magnetostriction plane and other in applied magnetic field vs. magnetostriction plane as shown in Figure-2.9 and Figure-2.10 for comparing with the data predicted by the network model. In these plots, some of the data point for small magnetic field has shown very small negative magnetostriction. This negative magnetostriction will provide negative actuation, and negative magneto-mechanical coupling that may not be the desired in the actuator application. Since the value of magnetostriction is negligible for small magnetic field, this negative magnetostriction can be assumed as zero for the output of network.

2.2.3.3 Study on Learning Rate

The back-propagation algorithm provides an "approximation" to the trajectory in weight space computed by the method of steepest descent. The smaller we make the learning rate, the smaller will the changes to the synaptic weights, and hence smoother will be the trajectory in weight space. This improvement, however, is attained at the cost of a slower rate of learning. If, on the other hand, we make the learning rate too large in order to speed up the rate of learning, the resulting large changes in the synaptic weights assume such a form that the network may become unstable (i.e. oscillatory). A simple method of increasing the rate of learning yet avoiding the danger of instability is to consider a momentum term with the learning rate parameter. This momentum term will be the certain percentage of the increment of the previous step added to the present step. The incorporation of momentum in the back-propagation algorithm represents a minor modification to the weight update, yet it may have some beneficial effects on the learning behavior of the algorithm. The momentum term may also have the benefit of preventing the learning process from terminating in a shallow local minimum on the error surface.

2.2.3.4 Sequential Training Mode

Learning rate is varied from 0.1 to 0.7 at an interval of 0.1 to study its effect on the learning performance for a 4-nodded hidden layer network. These are plotted in Figure-2.11 and

Figure-2.12. Slow learning performance is observed for low learning rate parameter. In addition, it affects the validation error of the trained network.

2.2.3.5 Training by Batch Mode

Same network is then trained in batch mode for different learning rate parameter. These are shown in Figure-2.13 and Figure-2.14. From the Figure, we see that as the learning rate parameter is increased from 0.1 to 0.7, the training rate of the network also increased. As in the sequential mode, the validation error is also connected with the learning rate.

2.2.3.6 Momentum Effect

Effect of momentum is also studied in the batch mode training with different momentum parameter, which means that certain percentage of the previous weight-increment is added to the present weight-increment. The effect of momentum on the overall training process is shown in Figure-2.15 and Figure-2.16. In the Figure-2.15, it is shown that at to higher value of learning rate parameter (0.8), the network is not trained properly and it becomes oscillatory in initial stage of learning. Figure-2.16 gives the training performance with different values of momentum from 0.1 to 0.7 with the same (0.8) learning rate parameter.

2.2.3.7 Selected Network

Based on the performance of the 3-layer network, following are the configuration that is used to obtain the constitutive model. The input layer has two neuron (one for each input variable), one hidden layer of 4 neurons and one output layer of one neuron, which corresponds to one output variable, namely the magnetostriction. The network is trained using sequential mode of training. The finished ANN model is delineated through the connection weights between the input and hidden layers and between the hidden and output layers, which are listed in Table 2.2 and Table 2.3 respectively.

Standard logistic function $y = 1/(1 + e^{-1.7159v})$ is used in hidden layer as activation function with linear output layer. Input (stress and magnetic field) and output (magnetostriction) data are normalized for better performance of network as follows.

$$\sigma_n = \frac{(\sigma - \sigma_{mean})}{(max|\sigma| - \sigma_{mean})} \tag{2.6}$$

$$H_n = \frac{(H - H_{mean})}{(max|H| - H_{mean})} \tag{2.7}$$

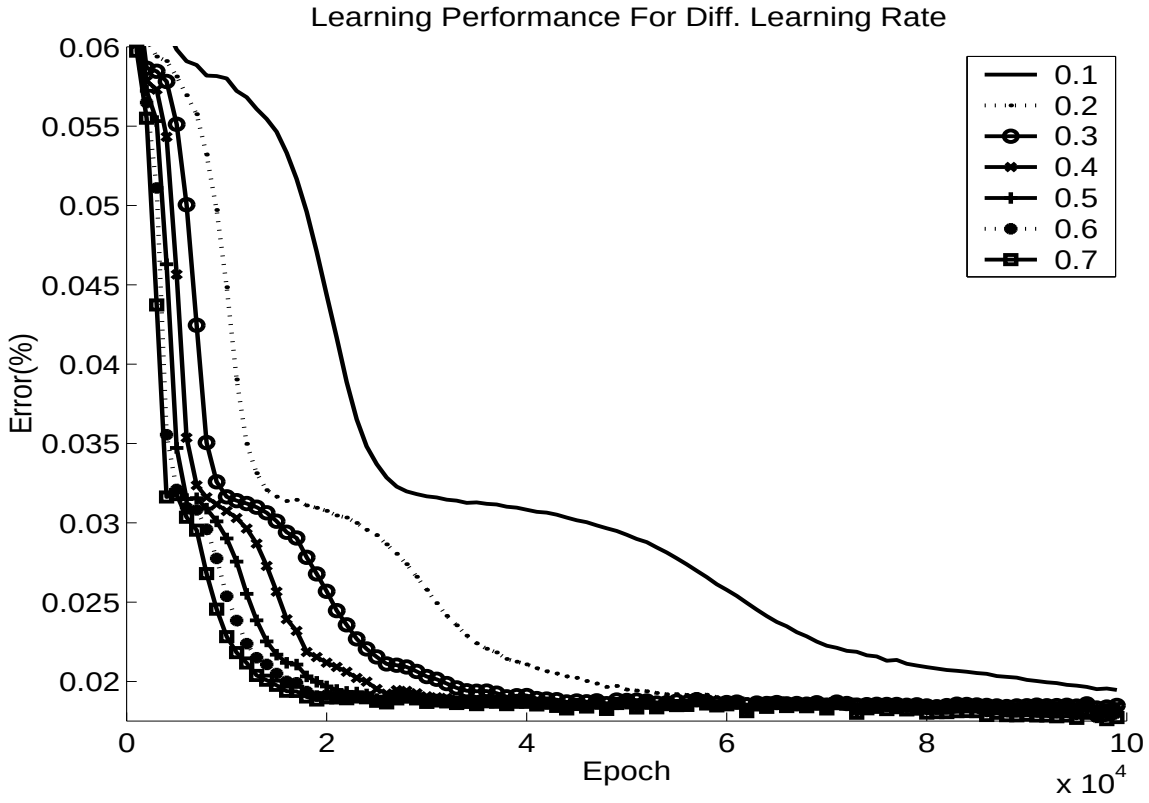

Figure 2.11: Effect of learning rate on training performance

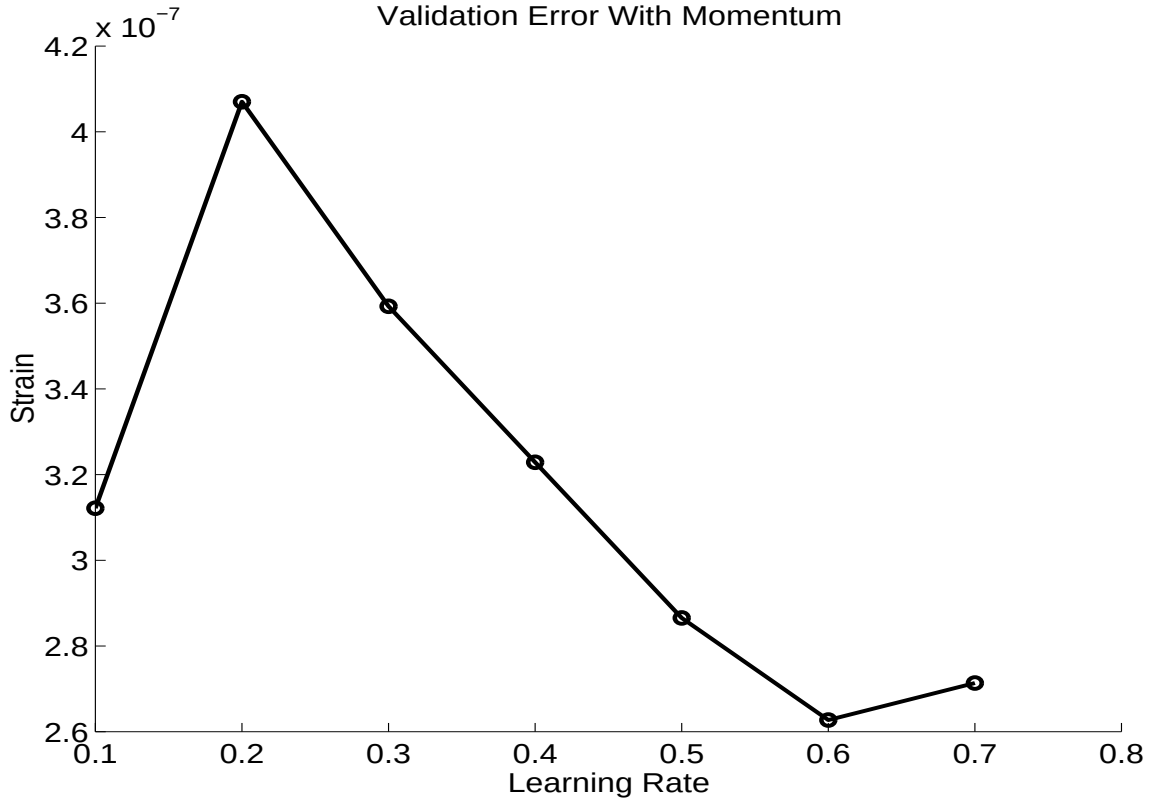

Figure 2.12: Effect of learning rate on validation performance

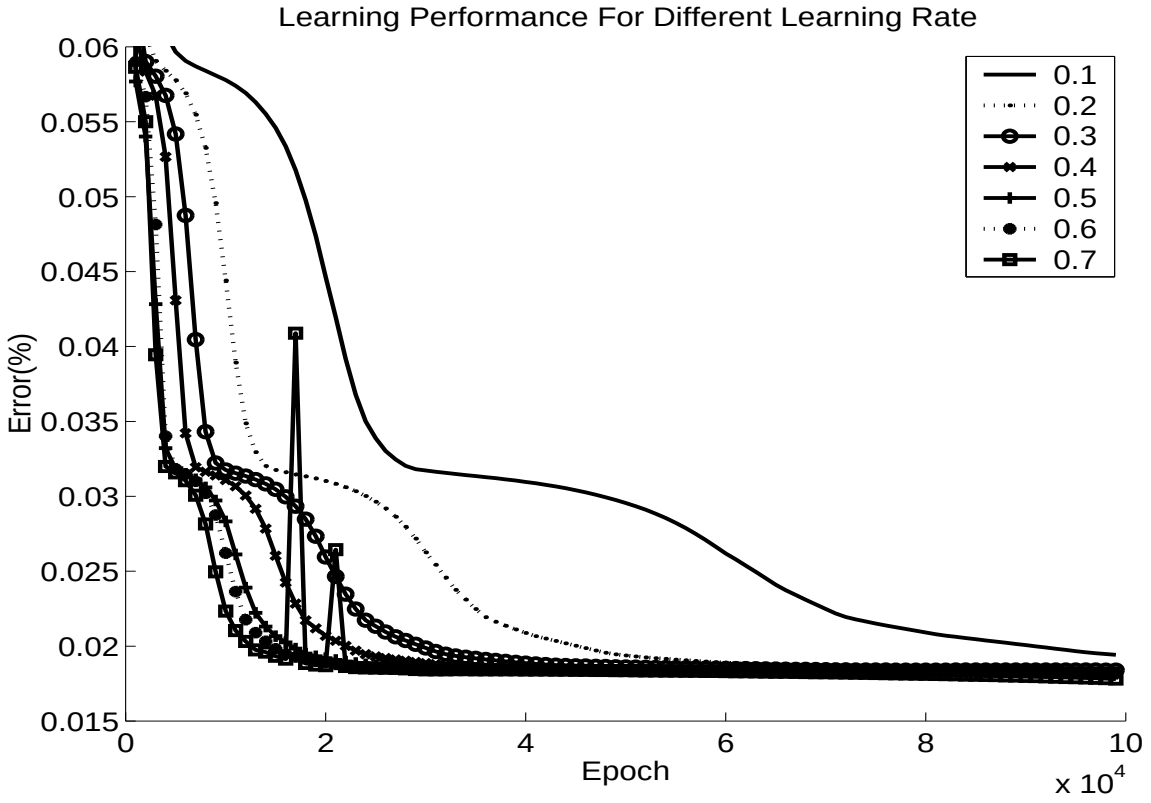

Figure 2.13: Effect of learning rate on batch mode training performance.

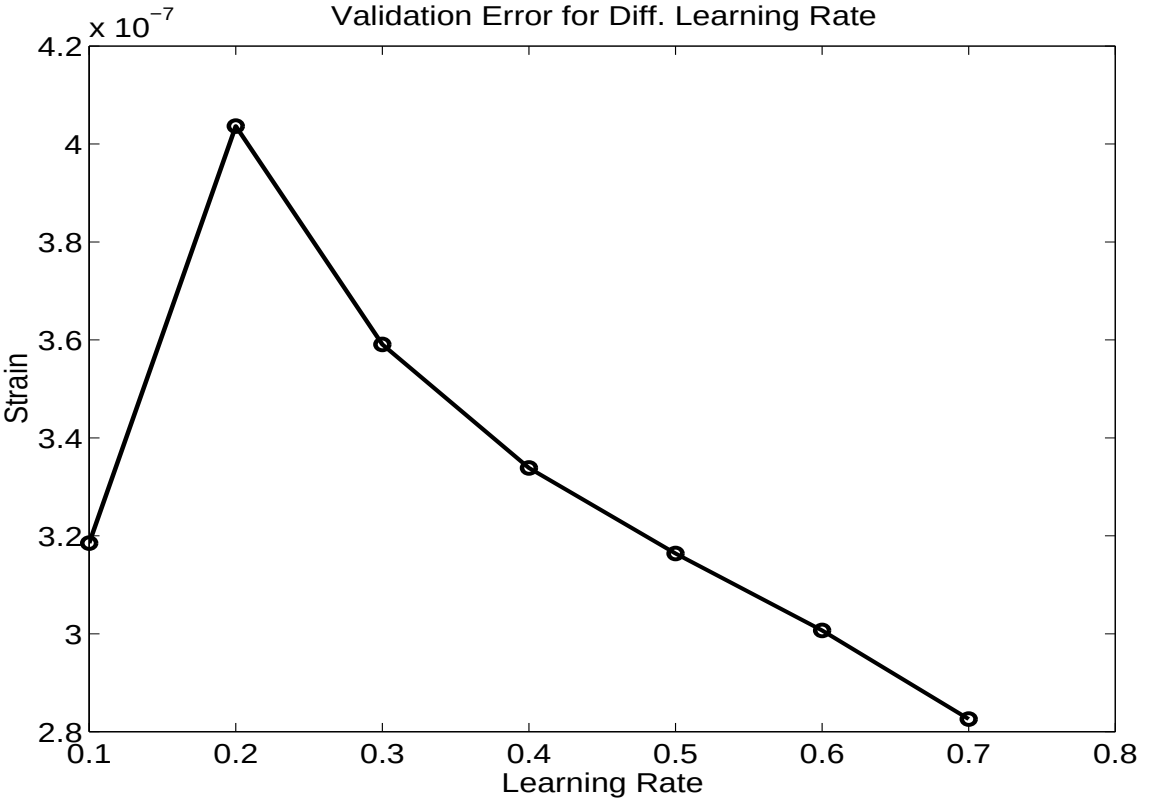

Figure 2.14: Effect of learning rate on validation performance for batch mode learning.

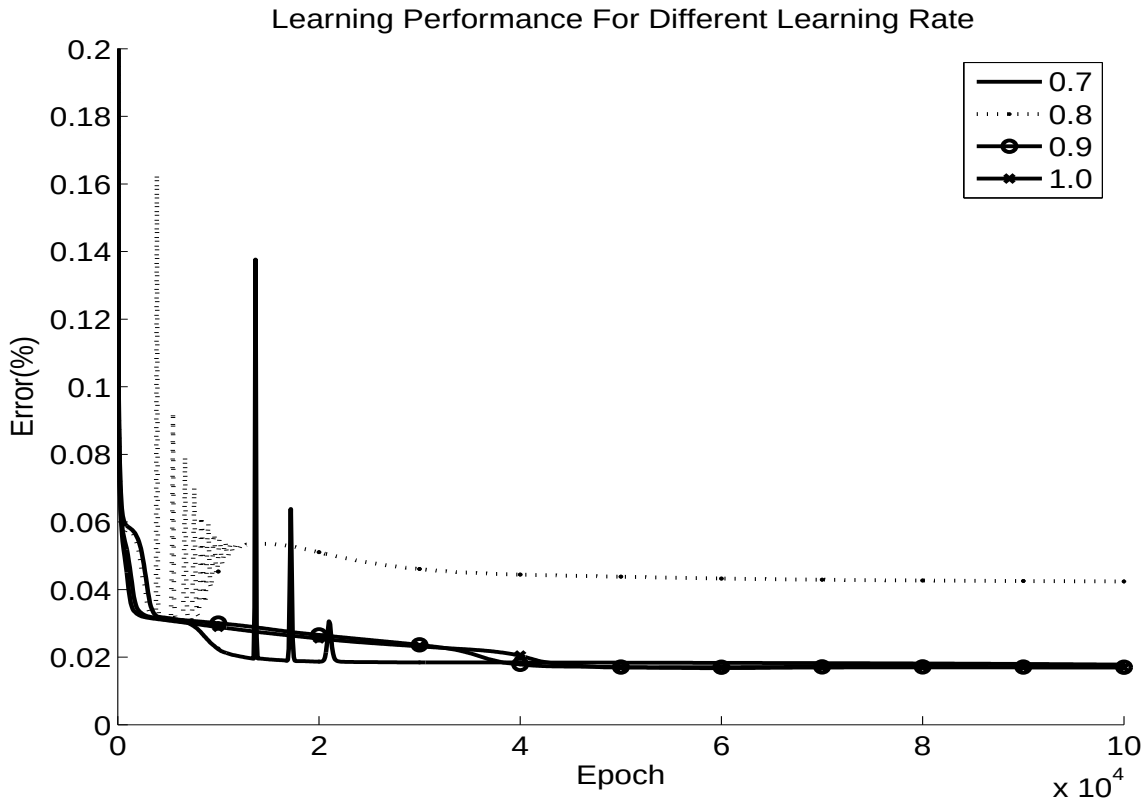

Figure 2.15: Effect of momentum on training performance.

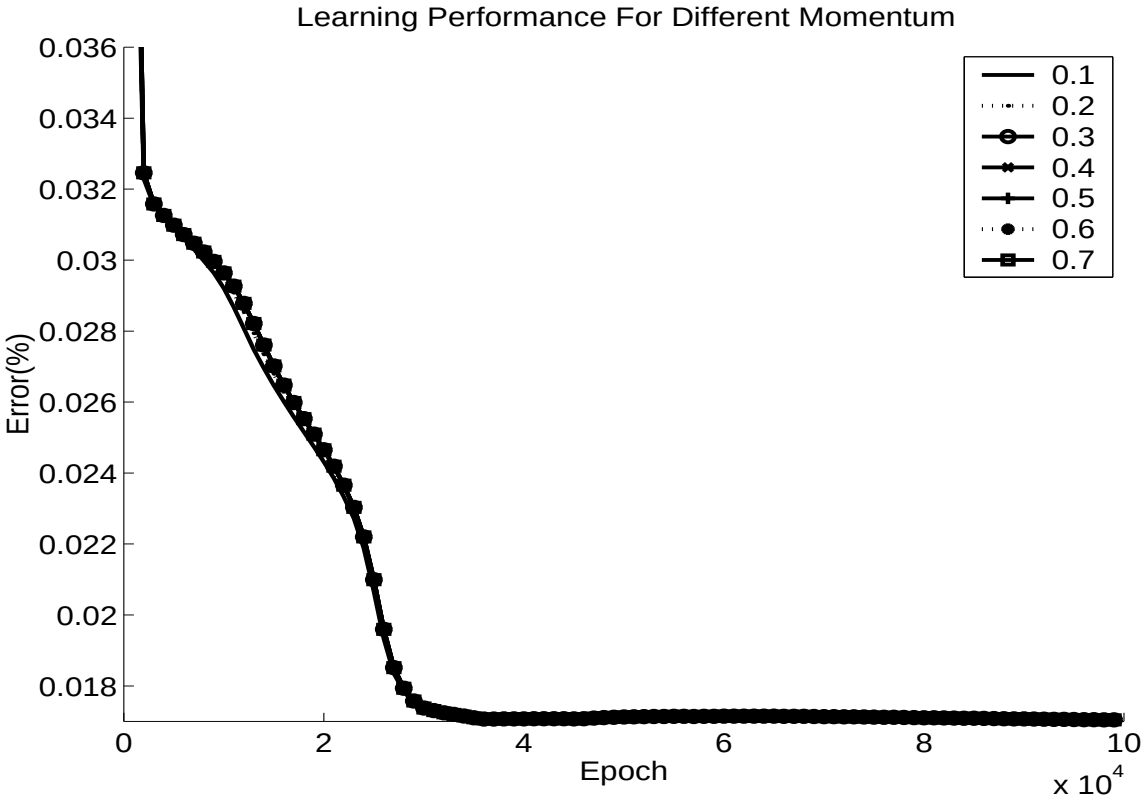

Figure 2.16: Effect of momentum on training performance.

$$\lambda_n = \frac{(\lambda - \lambda_{mean})}{(max|\lambda| - \lambda_{mean})} \tag{2.8}$$

In Equation-(2.6), σ_n is the normalized stress and σ_{mean} is mean stress of training samples. The value of σ_{mean} and $(max|\sigma| - \sigma_{mean})$ are $1.5243X10^7$ and $8.857X10^6$ Pa respectively. Similarly H_n is normalized magnetic field, H_{mean} is mean magnetic field of training samples. The value of H_{mean} and $(max|H| - H_{mean})$ in Equation-(2.7) are both 652 Oe. Normalized magnetostriction λ_n is the output of network, from which magnetostriction is calculated using Equation-(2.8). Where the value of λ_{mean} and $(max|\lambda| - \lambda_{mean})$ are both $0.798X10^{-3}$.

Table 2.2: Connection between input layer and hidden layer.

Hidden Layer Nodes	1	2	3	4
σ_n	-.11946E+01	-.33016E+00	.14013E+01	.14978E+01
H_n	.29959E+01	-.28768E+00	-.15922E+01	.19209E+00
Input Bias	.128112E+01	-.680953E+00	-.916353E-02	.187534E+01

Table 2.3: Connection between hidden layer and output layer.

Hidden Layer Nodes	1	2	3	4	output bias
λ_n	1.1240	-.65999	-.63945	1.0767	-1.27577

Figure-2.17 and Figure-2.18 gives the magnetostriction and magneto-mechanical coupling coefficient for different stress level (from 6.9MPa to 24.1 MPa) according to the present neural network model. As the network is trained taking data from all the stress level given in the manual [52], and the network is not validated for different stress level not given in the manual, there is a possibility of over training of network in other stress level. Networks become over trained while modelling noises in the responses, which are not desirable. However, by looking at the output of network for twenty intermediate stress level shown in these figures, it can be concluded that the network is not over trained.

2.2.4 Comparative Study with Polynomial Representation

Earlier study to model nonlinear actuation of magnetostrictive material was done considering a fourth order polynomial of magnetic field for each stress level [192]. The fourth order polynomial representation of magnetostriction required five real parameters for each curve represented in each stress level. To compute the magnetostriction from a

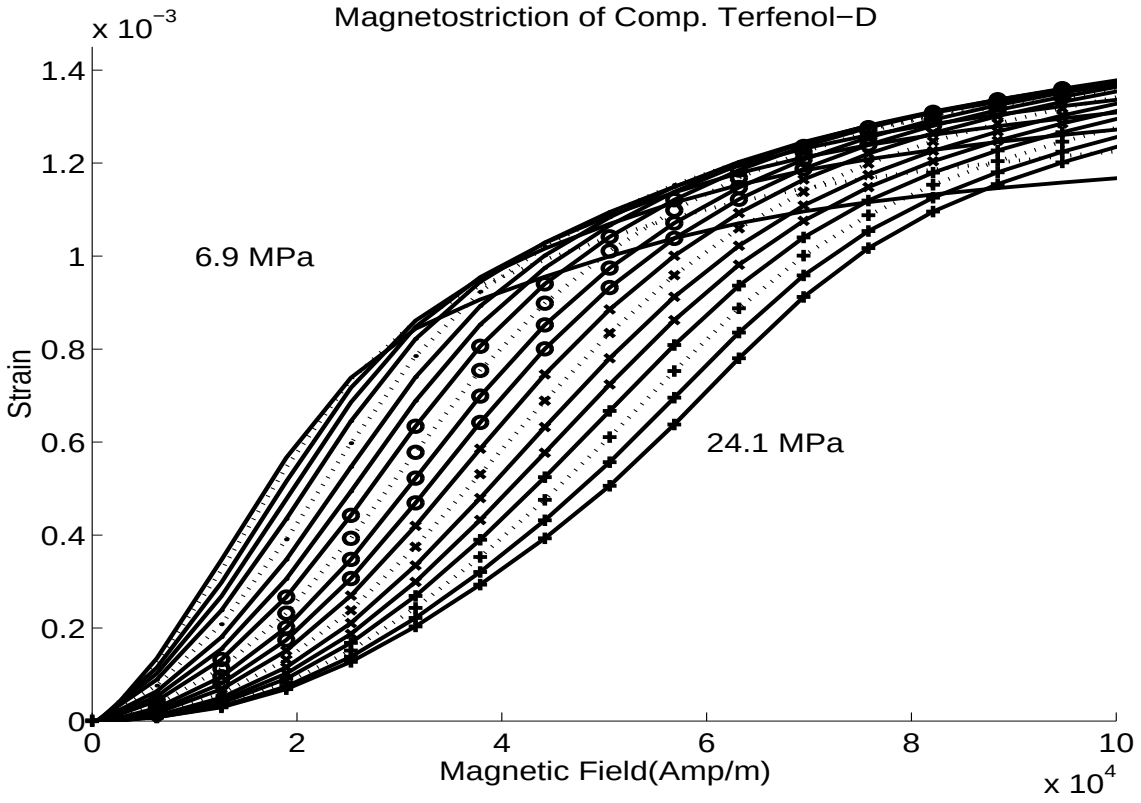

Figure 2.17: Magnetostriction for different stress level.

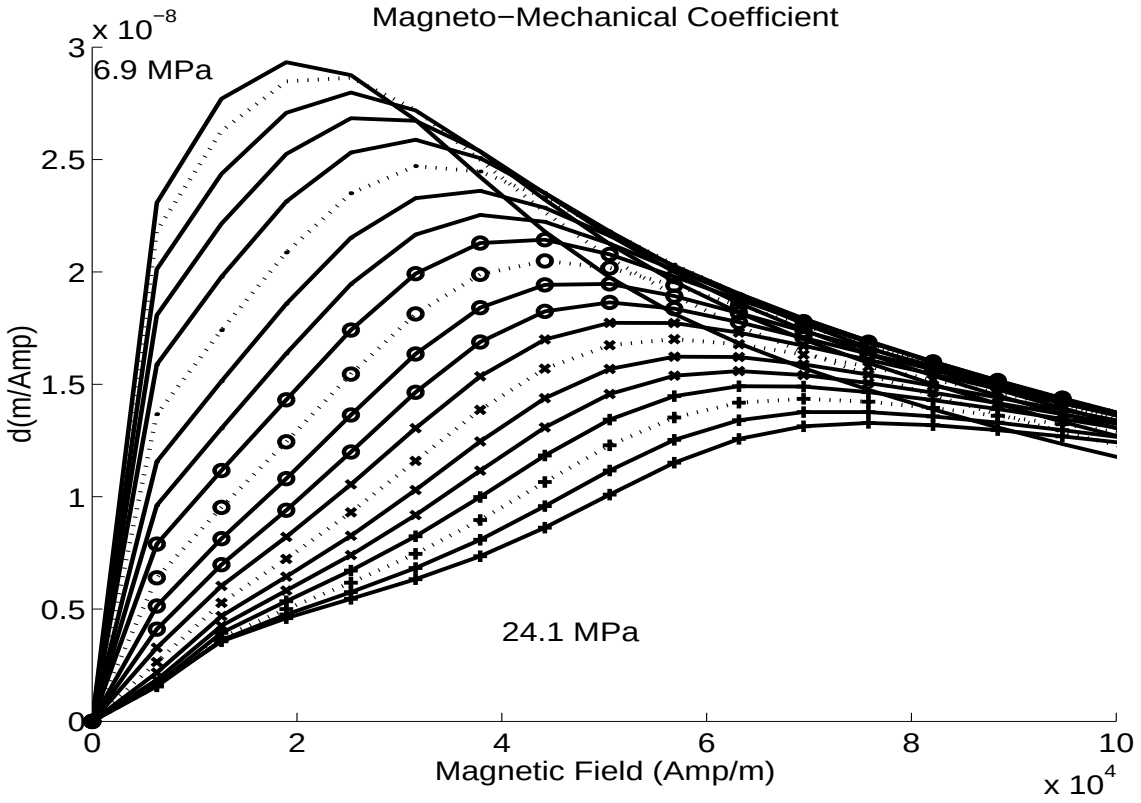

Figure 2.18: Coupling coefficient for different stress level.

specified curve, four floating-point multiplications and four floating-point additions are required. In addition, polynomial representation required interpolation of magnetostriction for the stress level that has no curve. This requires searching of upper and lower stress level for those where the polynomial representation is available and using these, magnetostriction can be computed using appropriate interpolation.

In this work, we use ANN to compute the magnetostriction, especially for nonlinear magnetostrictive model. The number of floating point operation required for a N nodded hidden layer network can be assessed as follows. The three layer network considered is represented by $3N$ number of weight parameters, $N + 1$ number of bias parameters and six numbers of normalization parameters. The input layer has two input node and output layer has one. Both input and the output is normalized. Total number of floating point operations required for N-nodded network is N number of division, N number of exponential computation, $4N+3$ number of multiplication and $4N+3$ number of addition. For four-nodded hidden layer network, 23 real parameters are required.

Some of the advantages of ANN over polynomial representation are as follows. In polynomial representation, if the number of curves are more, searching and storage requirement are also more compared to the artificial network model, although the requirement of floating point operations is less in polynomial representation. Another advantage in using artificial neural network over polynomial representation is that it has a direct representation of magnetostriction for a given applied magnetic field and stress level. As opposed to this, validation of the polynomial representation is not studied with different set of sample data apart from interpolated data. Magnetostriction according to artificial neural network (ANN), polynomial approach and experimental data is shown in Figure-2.19 for stress levels of 6.9, 15.1 and 24.1 MPa. For these stress levels, we see that there is a good match from all these approaches. For low stress level, in low and high magnetic fields, polynomial approach gives 50 and 100 ppm errors with experimental results, respectively. For all stress levels ANN approach gives with in 10 ppm errors in magnetostriction from experimental results.

2.3 Coupled Constitutive Model

As mention earlier, analysis of smart structures using magnetostrictive materials as either sensors or actuators has traditionally been performed using uncoupled models. Uncoupled models make the assumption that the magnetic field within the magnetostrictive material is constant and proportional to the electric coil current times the number of coil turn per

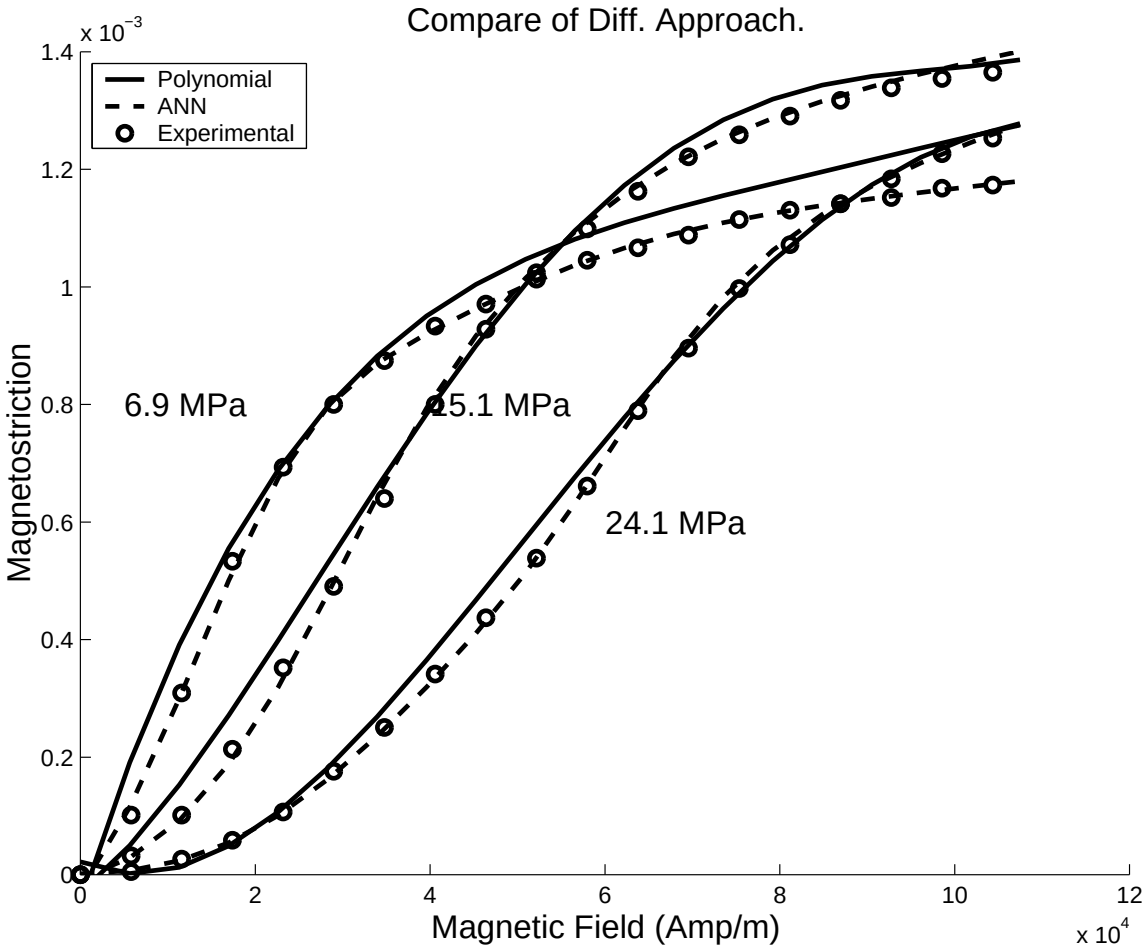

Figure 2.19: Magnetostriction for different stress level.

unit length. Hence actuation and sensing problems are solved by two uncoupled equations, which are given by the last part of Equation-(2.1) and Equation-(2.2), respectively. This makes the analysis relatively simple; however this method has its limitations. It is quite well known that [**S**], [**d**] and [μ] all depend on stress level and magnetic field. In the presence of mechanical loads, the stress changes and so is the magnetic field. Estimating the constitutive properties using uncoupled model in such cases will give inaccurate predictions. Hence, the constitutive model should be represented by a pair of coupled equations given by Equations-(2.1) & (2.2) to predict the mechanical and magnetic response. It is therefore necessary to simultaneously solve for both the magnetic response as well as the mechanical response regardless of whether the magnetostrictive material is being used as a sensor or actuator. Due to in-built non-linearity, the uncoupled model may not be

capable of handling certain applications such as (1) modelling passive damping circuits in vibration control and (2) development of self-sensing actuators in structural health monitoring. In these applications, the coupled equations require to be solved simultaneously. The solution of coupled equations simultaneously is a necessity for general-purpose analysis of adaptive structures built in with magnetostrictive materials. In general, the errors that result from using uncoupled models, as opposed to coupled ones, are problem dependent. There are some cases where very large differences exist in situations, where an uncoupled model is used over a coupled model [132].

In this work, the coupled case is analyzed with both linear and non-linear model. In linear-coupled model, magneto-mechanical coefficient, elasticity matrix and permeability matrix are assumed as constant. In nonlinear-coupled model, mechanical and magnetic nonlinearity are decoupled in their respective domains. The nonlinear stress-strain relationship is generally represented by modulus of elasticity and the nonlinear magnetic flux-magnetic field relationship represented by permeability of the material. Magneto-mechanical coupling coefficient will be assumed as constant in this case.

2.3.1 Linear Model

From Equation-(2.1) and Equation-(2.2), the 3D constitutive model for the magnetostrictive material can be written as

$$\{\sigma\} = [Q]\{\epsilon\} - [e]^T\{H\} \tag{2.9}$$

$$\{B\} = [e]\{\epsilon\} + [\mu^\epsilon]\{H\} \tag{2.10}$$

Where [**Q**] is Elasticity matrix, which is the inverse of compliance matrix [**S**], $[\mu^\epsilon]$ is the permeability at constant strain. $[\mu^\epsilon]$ and [**e**] are related to [**Q**] through

$$[e] = [d][Q] \tag{2.11}$$

$$[\mu^\epsilon] = [\mu^\sigma] - [d][Q][d]^T \tag{2.12}$$

For ordinary magnetic materials, where magnetostrictive coupling coefficients are zero, $[\mu^\epsilon]$=$[\mu^\sigma]$, the permeability.

Consider a magnetostrictive rod element of length L, area A, with Young modulus Q. If a tensile force F, is applied the rod develops a strain ϵ, and hence a stress σ. Total

strain energy in the rod will be

$$\begin{aligned} V_e &= \frac{1}{2}\int \epsilon\sigma dv = \frac{1}{2}\int \epsilon\{Q\epsilon - eH\}dv \\ &= \frac{1}{2}\int \epsilon Q\epsilon dv - \frac{1}{2}\int \epsilon eH dv \\ &= \frac{1}{2}ALQ\epsilon^2 - \frac{1}{2}ALe\epsilon H \end{aligned} \tag{2.13}$$

Magnetic potential energy in a magnetostrictive rod is

$$\begin{aligned} V_m &= \frac{1}{2}\int BH dv = \frac{1}{2}\int \{e\epsilon + \mu^\epsilon H\}H dv \\ &= \frac{1}{2}\int \epsilon eH dv + \frac{1}{2}\int H\mu^\epsilon H dv \\ &= \frac{1}{2}ALHe\epsilon + \frac{1}{2}AL\mu^\epsilon H^2 \end{aligned} \tag{2.14}$$

Magnetic external work done for N number of coil turn with coil current I is

$$W_m = IN\mu^\sigma HA \tag{2.15}$$

Mechanical External work done is

$$W_e = F\epsilon L \tag{2.16}$$

Total potential energy of the system becomes

$$\begin{aligned} T_p &= -\frac{1}{2}ALQ\epsilon^2 + \frac{1}{2}ALe\epsilon H \\ &\quad + \frac{1}{2}ALHe\epsilon + \frac{1}{2}AL\mu^\epsilon H^2 - IN\mu^\sigma HA + F\epsilon L \end{aligned} \tag{2.17}$$

Using Hamilton's Principle, $\delta(\int_{t_1}^{t^2} T_p\ dt) = 0$, two equations in terms of H and ϵ, will come.

$$-ALQ\epsilon + ALeH + FL = 0 \tag{2.18}$$

$$ALe\epsilon + ALH\mu^\epsilon - IN\mu^\sigma A = 0 \tag{2.19}$$

Dividing both equations by AL, equations will be

$$-Q\epsilon + eH = -\frac{F}{A} \tag{2.20}$$

$$e\epsilon + H\mu^{\epsilon} = \frac{IN\mu^{\sigma}}{L} \tag{2.21}$$

As right hand side of Equation-(2.21) is not function of ϵ and left hand side is magnetic flux density (Equation-(2.10)), it can be concluded that the magnetic flux density in this model is not function of ϵ. Hence, it is preserving the flux line continuity. Eliminating H from Equation-(2.20) and substituting this in Equation-(2.21), stress - strain relationship of the magnetostrictive material can be written as follows.

$$H = (Q\epsilon - F/A)/e \tag{2.22}$$

$$\epsilon = \frac{IN\mu^{\sigma}Ae + L\mu^{\epsilon}F}{ALe^2 + AL\mu^{\epsilon}Q} = \frac{IN\mu^{\sigma}eA + F\mu^{\epsilon}L}{AL\mu^{\sigma}Q} \tag{2.23}$$

From Equation-(2.23), total strain for applied coil current I and tensile stress F/A can be written as

$$\epsilon = \lambda + \epsilon_{\sigma} \tag{2.24}$$

where λ is the strain due to coil current, which is called the magnetostriction, and ϵ_{σ} is the strain due to tensile stress (elastic strain). These are given by

$$\lambda = \frac{IN\mu^{\sigma}Ae}{AL\mu^{\sigma}Q} = INd/L \tag{2.25}$$

$$\epsilon_{\sigma} = \frac{L\mu^{\epsilon}F}{AL\mu^{\sigma}Q} = \frac{F}{AQ^*} \tag{2.26}$$

Let Q^* be the modified elastic modulus and substituting the value of e and μ^{ϵ} from Equation-(2.11) and Equation-(2.12), Q^* will be

$$Q^* = \frac{Q\mu^{\sigma}}{\mu^{\epsilon}} = \frac{Q\mu^{\sigma}}{\mu^{\sigma} - d^2Q} = Q + \frac{e^2}{\mu^{\epsilon}} \tag{2.27}$$

If the value of μ^{σ} is much greater than d^2Q, μ^{ϵ} can be assumed equal to μ^{σ} and Q^* can be assumed as equal to Q. Hence, the total strain of the rod will be same as for the uncoupled model. The first term in the strain expression is the strain due to magnetic field, and the second term is the strain due to the applied mechanical loading. However, for Terfenol-D [52], the value of d^2Q is comparable with μ^{σ}. Substituting the value of strain from Equation-(2.23) in the Equation-(2.22), the value of magnetic field will be

$$H = -\frac{F}{Ae}(1 - \frac{\mu^{\epsilon}}{\mu^{\sigma}}) + \frac{IN}{L} \tag{2.28}$$

Note that although the magnetostriction value (INd/L) in Equation-(2.25) is same for coupled and uncoupled case, the value of magnetic field is different. Assuming r as the ratio of two permeabilities or two elastic module, from Equation-(2.27), r can be written as.

$$r = \frac{\mu^{\sigma}}{\mu^{\epsilon}} = \frac{Q^{*}}{Q} \tag{2.29}$$

If the value of r is one, result of coupled analysis is similar with uncoupled analysis. In Figure-2.20, the value of r is shown in contour plot for different values of constant strain permeability and modulus of elasticity considering coupling coefficient as $15X10^{-9}$ m/Amp. In the Figure-2.20(a), value of r is shown for different values of permeability and elastic modulus. In the Figure-2.20(b), value of r is shown for different values of permeability and modified elasticity. In these plots it is clear that for a particular value of elasticity, if the value of permeability increases, the value of r will decrease. However, for a particular value of permeability, if the value of elasticity increases the value of r will increase. In Figure-2.21, the value of r is shown in contour plot for different value of permeabilities and coupling coefficient considering module of elasticity as 15GPa. In Figure-2.21(a), value of r is given for different values of constant strain permeability and coupling coefficient. In Figure-2.21(b), value of r is shown for different values of constant stress permeability and coupling coefficients. In these plots it is clear that for a particular value of permeability, if the value of coupling coefficient increases the value of r will increase. But for a particular value of coupling coefficient if the value of permeability increases, the value of r will decrease. In Figure-2.22, the value of r is shown in contour plot for different value of elasticities and coupling coefficient considering constant strain permeability as $7X10^{-6}$ henry/m. In Figure-2.22(a), value of r is given for different values of modulus of elasticities and coupling coefficient. In Figure-2.22(b), value of r is shown for different values of modified elasticities and coupling coefficients. In these plots it is clear that for a particular value of elasticity, if the value of coupling coefficient increases the value of r will increase. Similarly, for a particular value of coupling coefficient if the value of elasticity increases, the value of r will increase.

From experimental data given in Etrema manual [52], the best value of Q, μ^{σ} and d is calculated, which will minimize the difference between experimental data and the data according to Equation-(2.23) by least square approach. In the first set of experimental data, only magnetostriction value is reported, which is expressed in Equation-(2.25). The

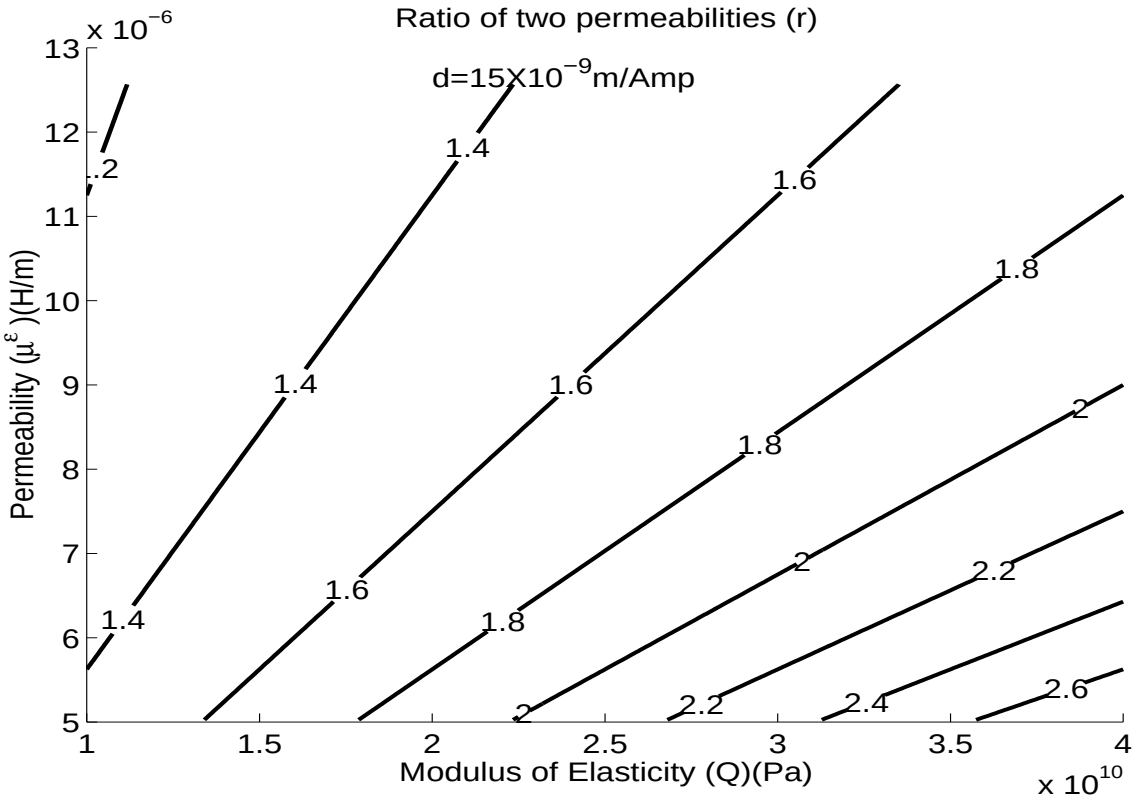

(a)

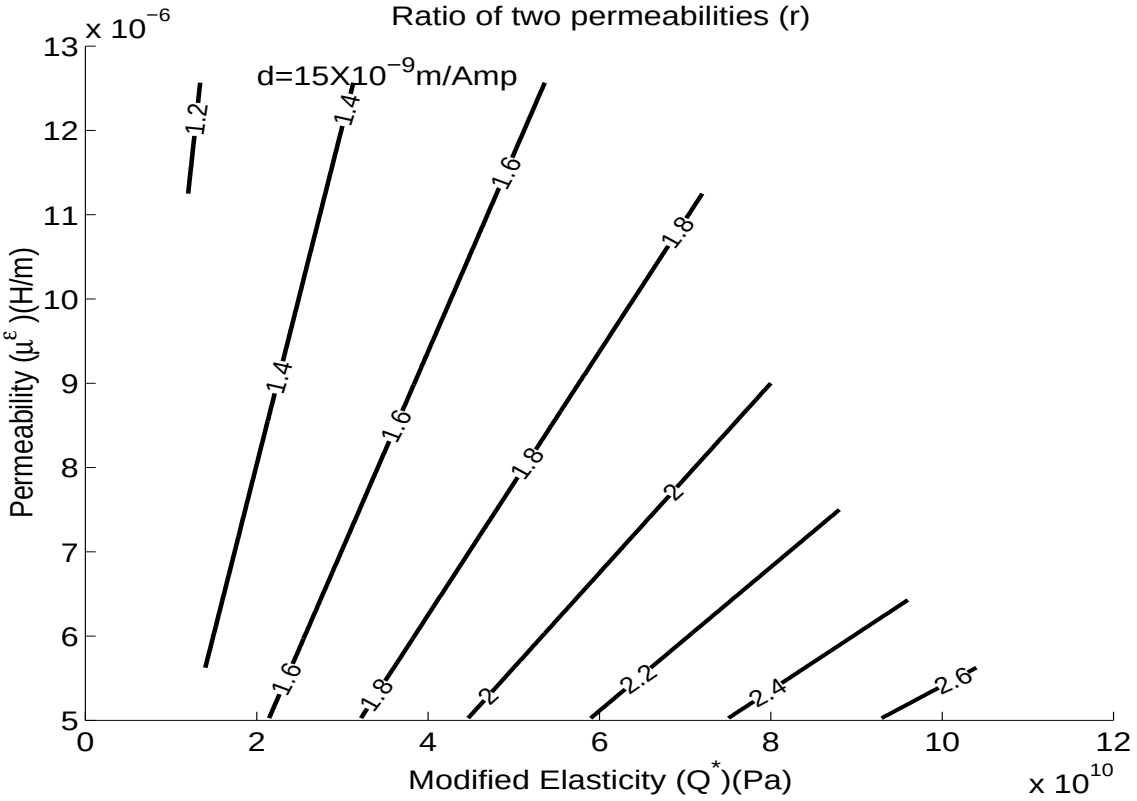

(b)

Figure 2.20: Ratio of two permeabilities (r) with different values of permeability vs. modulus of elasticity (a) and modified elasticity (b), considering d=$15X10^{-9}$ m/Amp .

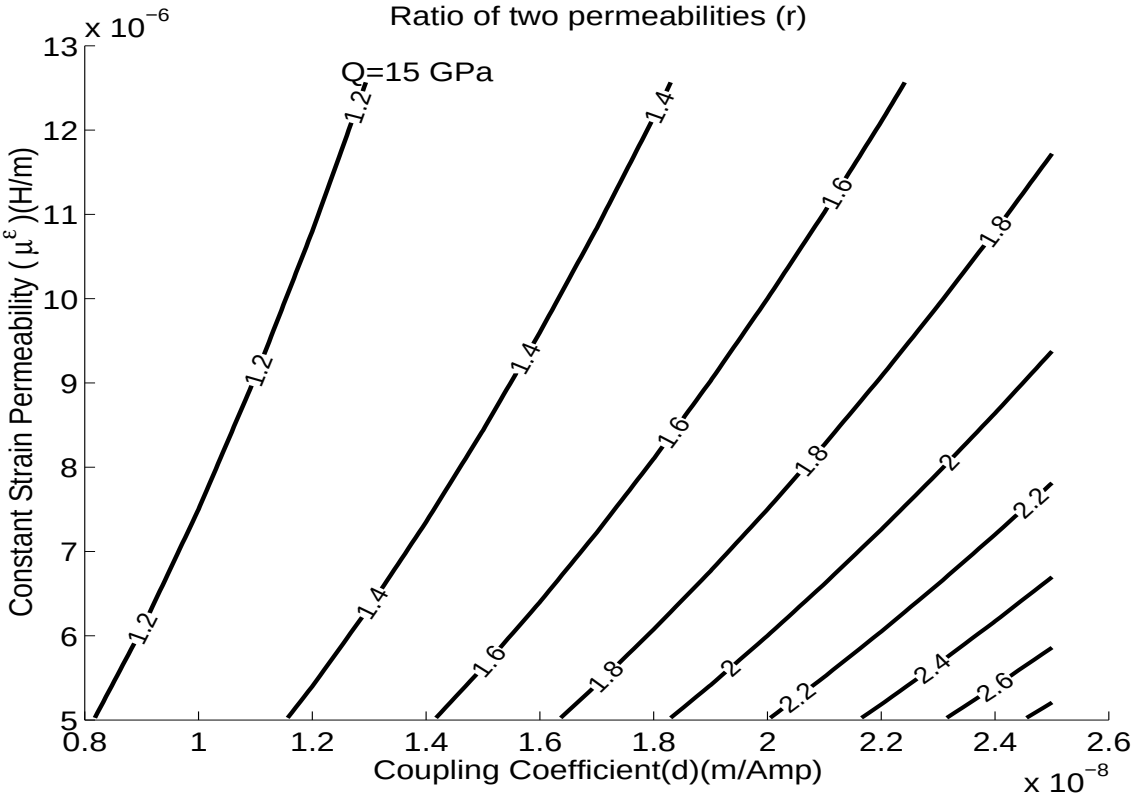

(a)

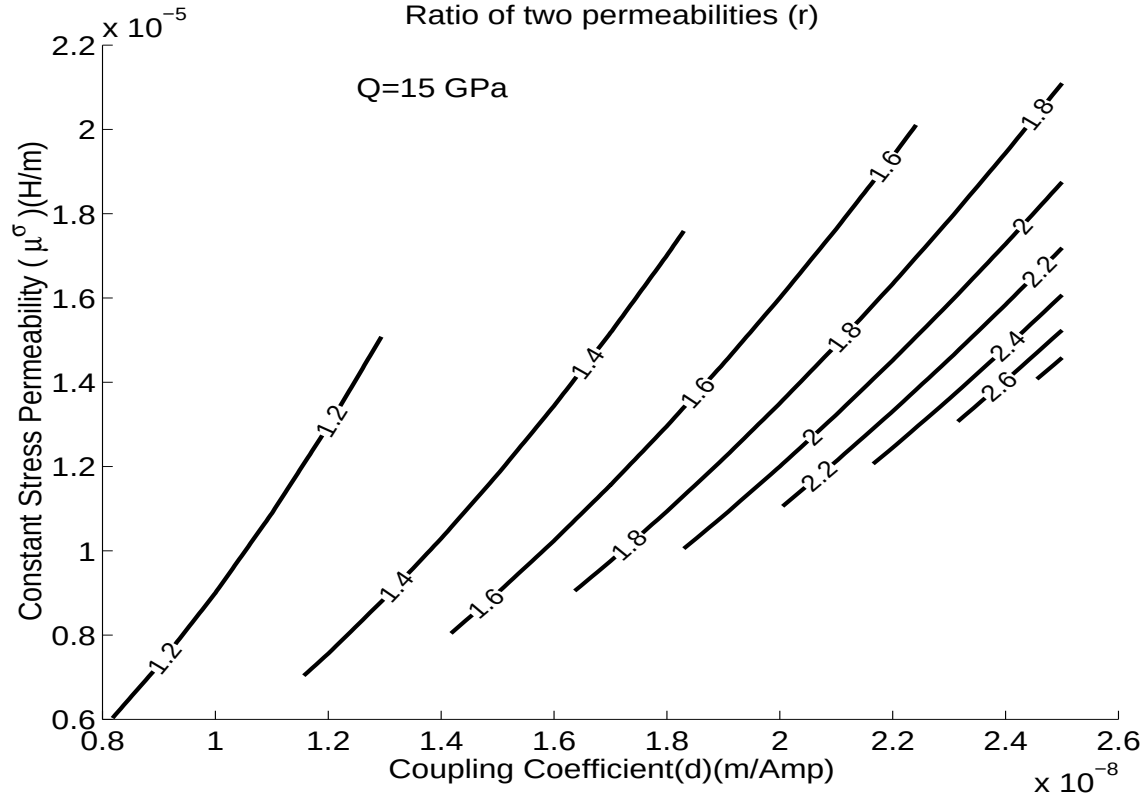

(b)

Figure 2.21: Ratio of two permeabilities (r) with different values of coupling coefficient vs. constant strain permeability (a) and constant stress permeability (b), considering Q=15GPa.

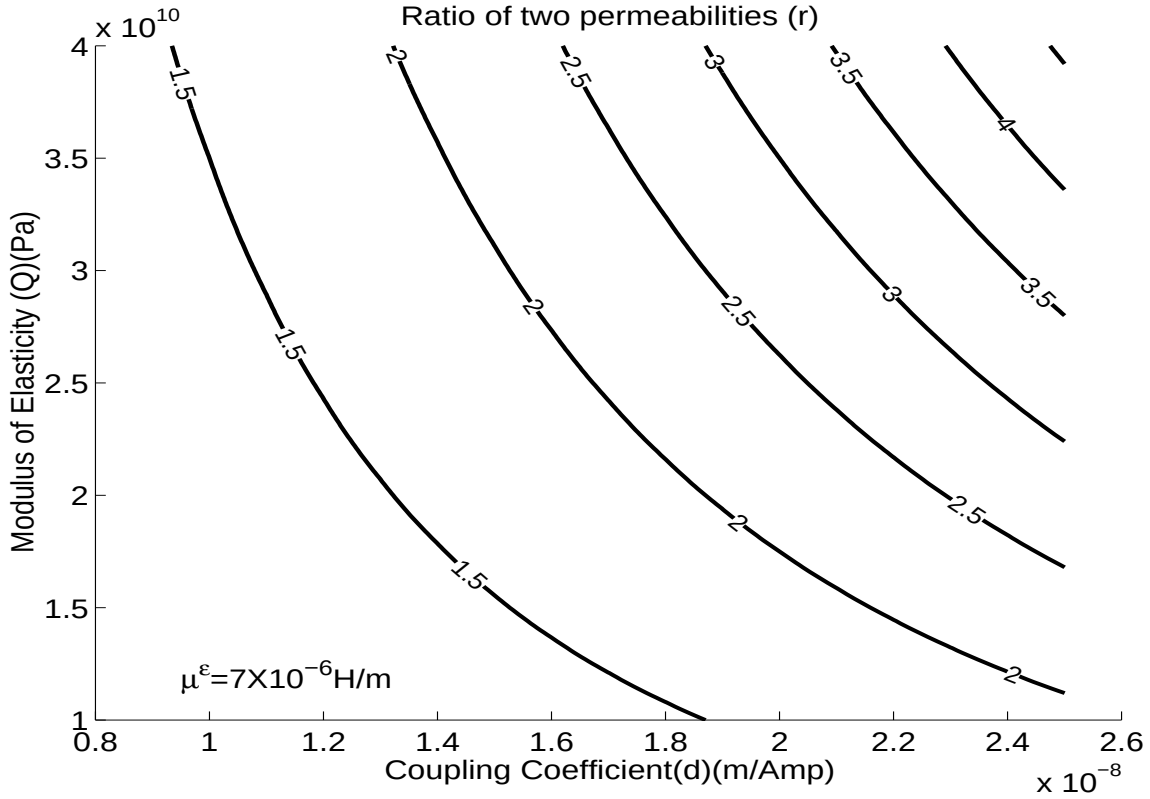

(a)

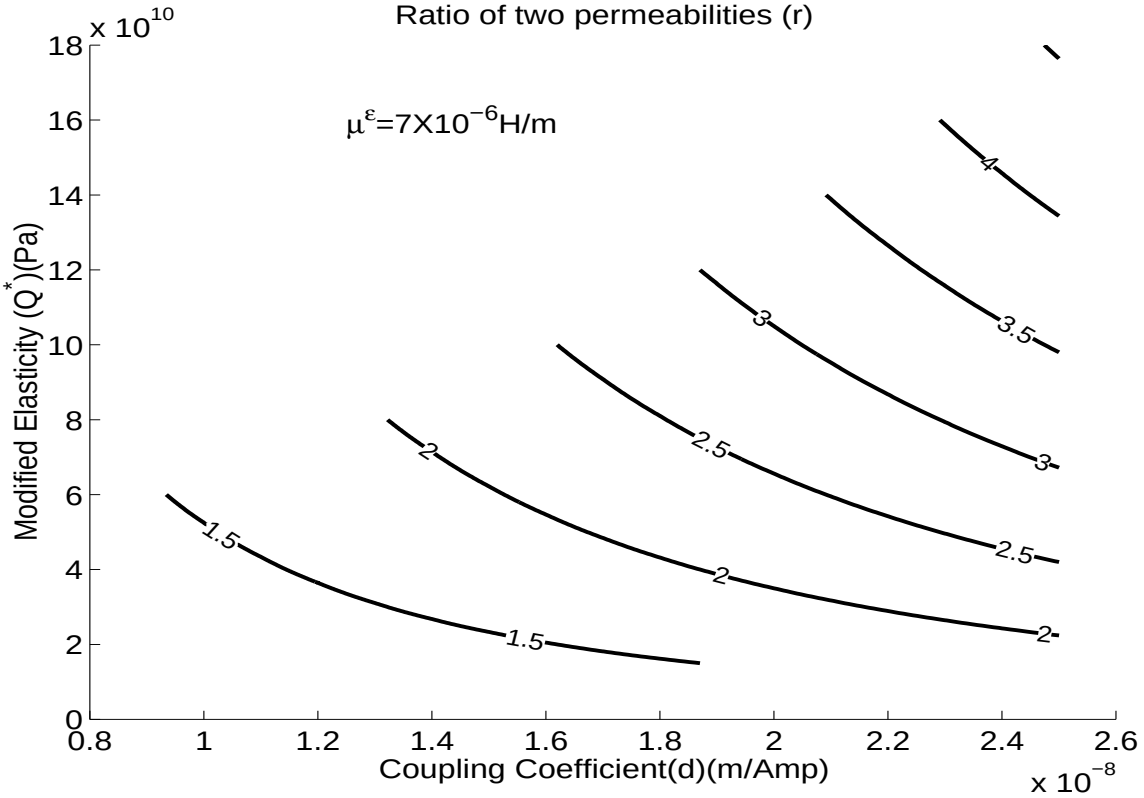

(b)

Figure 2.22: Ratio of two permeabilities (r) with different values of coupling coefficient vs. modulus of elasticity (a) and modified elasticity (b), considering $\mu^{\epsilon} = 7X10^{-6}$ henry/m.

value of coupling coefficient is calculated minimizing the total square error, λ_{Error}.

$$\lambda_{Error} = \sum (\lambda_{exp} - \lambda)^2 \tag{2.30}$$

Similarly in the second set of experimental data, strain due to compressive stress (ϵ_σ) is reported. The expression for the value of elastic strain, ϵ_σ is given in Equation-(2.26). In this expression, the value of Q^* is calculated minimizing the total square error ϵ_σ^{Error}.

$$\epsilon_\sigma^{Error} = \sum (\epsilon_\sigma^{exp} - \epsilon_\sigma)^2 \tag{2.31}$$

From Equation-(2.30), using first set of experimental data (plotted in Figure-2.1), the value of d is calculated as $14.8X10^{-9}$ (m/amp). From Equation-(2.31), using the second set of experimental data (plotted in Figure-2.3), the value of Q^* is 33.4 GPa. Assuming constant strain permeability (μ^ϵ) of the material is $7X10^{-6}$ henry/m, the value of r is 1.6, constant stress permeability (μ^σ) is $11.2X10^{-6}$ henry/m and Q is 20.8 GPa. From these studies it is clear that for giant magnetostrictive material, like Terfenol-D, coupled analysis will give better result than uncoupled analysis. But for magnetostrictive material with low coupling coefficient, the uncoupled analysis will give similar result with coupled analysis.

The coupled linear model cannot model the high nonlinearity of magnetostriction λ, which is required for design of actuator. Even considering nonlinear magnetic (magnetic field-magnetic flux) and mechanical (stress-strain) relationships with linear coupling coefficient, nonlinear relationships of magnetostriction cannot be modelled as it is a function of coil current, coil turn per unit length of actuator and magneto-mechanical coefficient (Equation-(2.25)). In the next section, we introduce a nonlinear model with a constant coupling coefficient, which can model the non-linear constitutive model exactly for constant magnetic coupling.

2.3.2 Nonlinear Coupled Model

The model developed in this section is based on a coupled magneto-mechanical formulation, which allows accurate prediction of both the mechanical and the magnetic response of a magnetostrictive device with nonlinear magnetic and mechanical properties. Nonlinearity in this model is introduced using two nonlinear curves, one for stress-strain relation and the second for magnetic field-magnetic flux relation, which enables to decouple the non-linearity in mechanical and magnetic domains. Magneto-mechanical coefficient is considered as a real parameter scalar value. Two-way coupled magneto-mechanical theory

is used to model magnetostrictive material. The formulation starts with the constitutive relations. In earlier coupled-linear model, stress (σ) and magnetic flux density (B) was expressed as a function of the components of strain (ϵ) and magnetic field (H) as per Equation-(2.9) and Equation-(2.10). Main draw back with such an approach is that the non-linearity between magnetic domain (μ^ϵ) and mechanical domain (Q) are not uncoupled. Hence, it is difficult to model non-linearity in earlier representation. To address these issues, a different approach is used in which Equation-(2.9) and Equation-(2.10) are rearranged in terms of the mechanical strain (ϵ) and the magnetic flux density (B). In doing so, the mechanical non-linearity is limited to stress-strain relationship and magnetic non-linearity is limited to magnetic field-magnetic flux relationship.

One-dimensional nonlinear modelling is again studied using one-dimensional experimental data from Etrema manual. The constitutive equation can now be rewritten in terms of magnetic flux density (B) and strain (ϵ), as

$$\sigma = E\epsilon - f^T B \tag{2.32}$$

$$H = -f\epsilon + gB \tag{2.33}$$

Where

$$\begin{aligned} g &= (\mu^\epsilon)^{-1} \\ f &= gdQ = e/\mu^\epsilon \\ E &= Q + Qdf = Q^* \end{aligned} \tag{2.34}$$

Like linear case, we will again consider a magnetostrictive rod element of length L, area A, applied tensile force F, strain ϵ, stress σ, elastic modulus E. Total strain energy in the rod will be

$$\begin{aligned} V_e &= \frac{1}{2}AL\epsilon\sigma = \frac{1}{2}\epsilon(E\epsilon - fB) \\ &= \frac{1}{2}ALE\epsilon^2 - \frac{1}{2}AL\epsilon fB \end{aligned} \tag{2.35}$$

Magnetic potential energy in magnetostrictive rod is given by

$$\begin{aligned} V_m &= \frac{1}{2}ALBH = \frac{1}{2}AL(-f\epsilon + gB)B \\ &= -\frac{1}{2}ALBf\epsilon + \frac{1}{2}ALgB^2 \end{aligned} \tag{2.36}$$

Magnetic external work done for N turn coil with coil current I is

$$W_m = INBA \tag{2.37}$$

Mechanical External work done is

$$W_e = F\epsilon L \tag{2.38}$$

Total potential energy of the system is equal to $Tp = -Ve - Vm + Wm + We$.

$$T_p = -\frac{1}{2}ALE\epsilon^2 + AL\epsilon fB - \frac{1}{2}ALgB^2 + INBA + F\epsilon L \tag{2.39}$$

Using Hamilton's Principle, two equations of B and ϵ will be

$$-ALE\epsilon + ALfB + FL = 0 \tag{2.40}$$

$$AL\epsilon f - ALgB + INA = 0 \tag{2.41}$$

Dividing by the Volume, AL, Equation-(2.40) and Equation-(2.41) will become

$$E\epsilon - fB = \frac{F}{A} \tag{2.42}$$

$$-f\epsilon + gB = \frac{IN}{L} \tag{2.43}$$

Eliminating B from Equation-(2.42) and substituting this in Equation-(2.43), stress-strain relationship for the magnetostrictive material can be obtained as

$$B = \frac{E\epsilon - F/A}{f} \tag{2.44}$$

$$\epsilon = \frac{F/A + INf/(gL)}{E - f^2/g} \tag{2.45}$$

Assuming E^* as the magnetically free elastic modulus

$$E^* = E - f^2/g = Q \tag{2.46}$$

Total strain for applied coil current I and tensile force, F will be

$$\epsilon = \frac{INf}{(gLE^*)} + \frac{F}{AE^*} \tag{2.47}$$

Here $E = Q^*$ is the elastic modulus for a magnetically stiffened rod and $Q = E^*$ is for magnetically flexible rod. Magnetically stiffened means that the magnetic flux *B=0* inside the rod as rod is wound by short circuited coils. Magnetically flexible means the rod is free from any coil. *E-Q* relation can be obtained form Equation-(2.34).

To model the one-dimensional nonlinear magnetostrictive stress-strain and magnetic field-magnetic flux relationships, Equation-(2.32) and Equation-(2.33) can be written as,

$$E(\epsilon) - fB = \sigma \tag{2.48}$$

$$-f\epsilon + g(B) = \frac{IN}{L} \tag{2.49}$$

where f is the real parameter of scalar value, and ϵ - $E(\epsilon)$, B - $g(B)$ are two real parameter nonlinear curves. The basic advantage of this model is that only two nonlinear curves are required for representing nonlinearity reported in different stress levels. As opposed to this approach, in straight forward polynomial representation of magnetostriction [192], one requires single nonlinear curve for every stress level. To get the coefficients of two nonlinear curves and the value of real parameter f, experimental data from Etrema manual [52] is used. From strain, applied coil current and stress level available in the manual, these coefficients are evaluated. Considering modulus elasticity as 30GPa, and f as $75.3X10^6$ m/Amp as an initial guess, the values of magnetic flux density, B are calculated from Equation-(2.48). Similarly from Equation-(2.49), values of $g(B)$ are evaluated. From these B and $g(B)$ values, curves of $B - g(B)$ is computed. This curve is used to get mechanical relationship. Here, the value of B is computed from $B - g(B)$ relationship. From this value of B, using Equation-(2.48), values of $E(\epsilon)$ is calculated. From the $E(\epsilon)$ and ϵ values, the mechanical nonlinear curve of $\epsilon - E(\epsilon)$ relationship is computed. In summery, first the magnetic nonlinear curve is evaluated from mechanical nonlinear curve and mechanical nonlinear curve is evaluated from magnetic nonlinear curve with the help of experimental data given in Etrema manual [52]. This iteration will continue till both mechanical curve and magnetic curve converges. Thus, with the help of experimental data given in Etrema manual [52] and Equations-(2.48) and (2.49), nonlinear mechanical and magnetic relationship is evaluated. Initial values of modulus of elasticity and f are computed on trial and error basis.

For sensor device, where coil current is assumed as zero, strain and the value of magnetic flux due to the application of stress is given by

$$\epsilon = \frac{g(B)}{f} \tag{2.50}$$

$$B = \frac{E(\epsilon) - \sigma}{f} \tag{2.51}$$

Nonlinear curves for magnetic and mechanical properties are shown in Figure-2.23. These two nonlinear curves are represented as sixth order polynomial given in Equation-(2.52) and Equation-(2.53). Coefficients of these polynomials curves are given in Table-2.4, where unit of B is tesla, $g(B)$ is Amp/m and $E(\epsilon)$ is Pa. The value of magneto-mechanical coupling parameter (f) is $75.3X10^6$ m/amp, which is reciprocal of $13.3X10^{-9}$ amp/m.

Table 2.4: Coefficients for sixth order polynomial.

	c	d	a	b
6	0	0	4.5419e+28	1.5853e-50
5	-2.1687e+06	-1.9526e-27	7.6602e+25	-6.1288e-44
4	1.5211e+06	1.1589e-21	-4.2662e+22	-1.0355e-34
3	3.5828e+05	-2.0047e-16	-6.6788e+19	-4.0508e-27
2	-2.1062e+05	2.0096e-12	2.3911e+16	1.0806e-19
1	2.2754e+05	4.7789e-06	1.2539e+13	2.7977e-11
0	-8.8129e+03	4.4239e-02	3.3893e+10	-1.9704e-05

$$\begin{aligned} g(B) &= c_5 * B^5 + .. + c_1 * B + c_0 \\ B &= d_5 * g(B)^5 + .. + d_1 * g(B) + d_0 \end{aligned} \tag{2.52}$$

$$\begin{aligned} E(\epsilon) &= a_6 * \epsilon^6 + .. + a_1 * \epsilon + a_0 \\ \epsilon &= b_6 * E(\epsilon)^6 + .. + b_1 * E(\epsilon) + b_0 \end{aligned} \tag{2.53}$$

On the basis of these two curves given in Equation-(2.52) and Equation-(2.53) and parameter (f), strain, magnetostriction vs. applied magnetic field for different stress level are plotted in Figure-2.24. The experimental data of strain-magnetic field relationships for different stress level is almost matching with this model. Similarly strain-compressive force and elastic modulus for different magnetic field level is plotted in Figure-2.25. Elastic modulus initially decreases and then increases for each magnetic field level, which is also reported in [52].

Computation of Flux and Strain from Coil Current and Stress: As two nonlinear curves are related in these relationships, the calculation of magnetic flux and strain from stress and coil current is an iterative procedure. Initially, the value of magnetic flux, B is assumed a certain value. From $B - g(B)$ curve, the value of $g(B)$ is evaluated. From

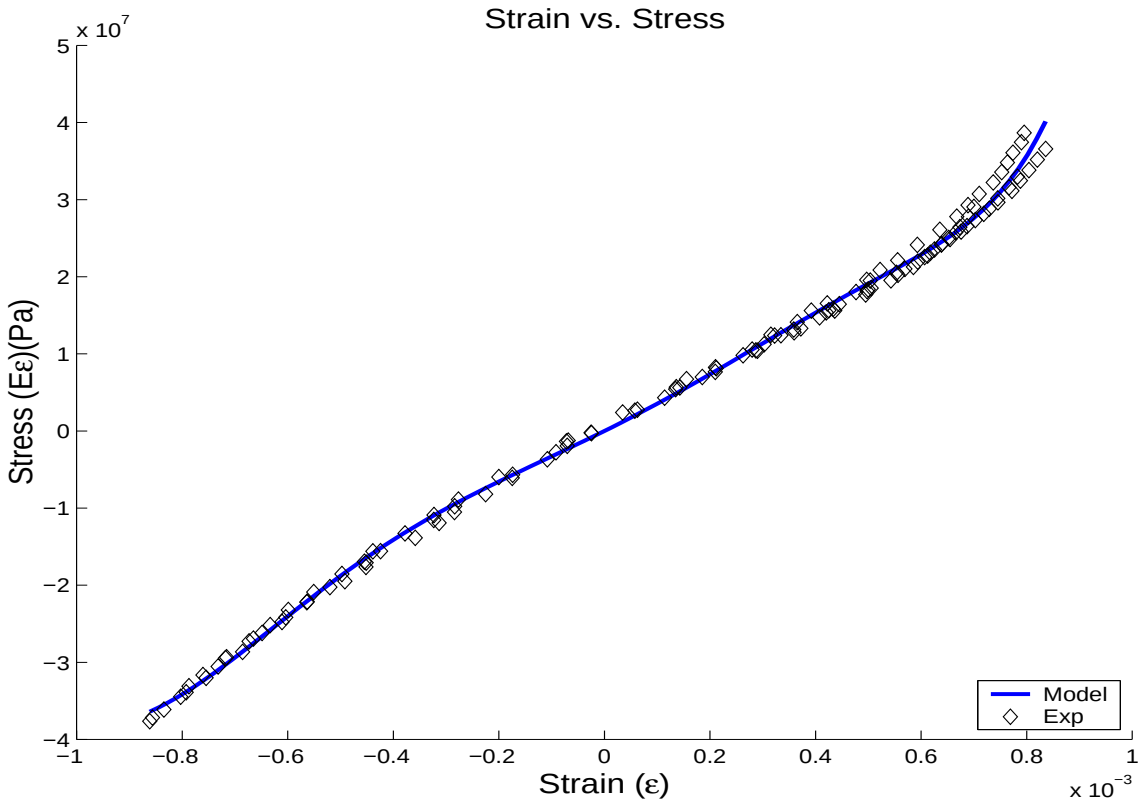

(a)

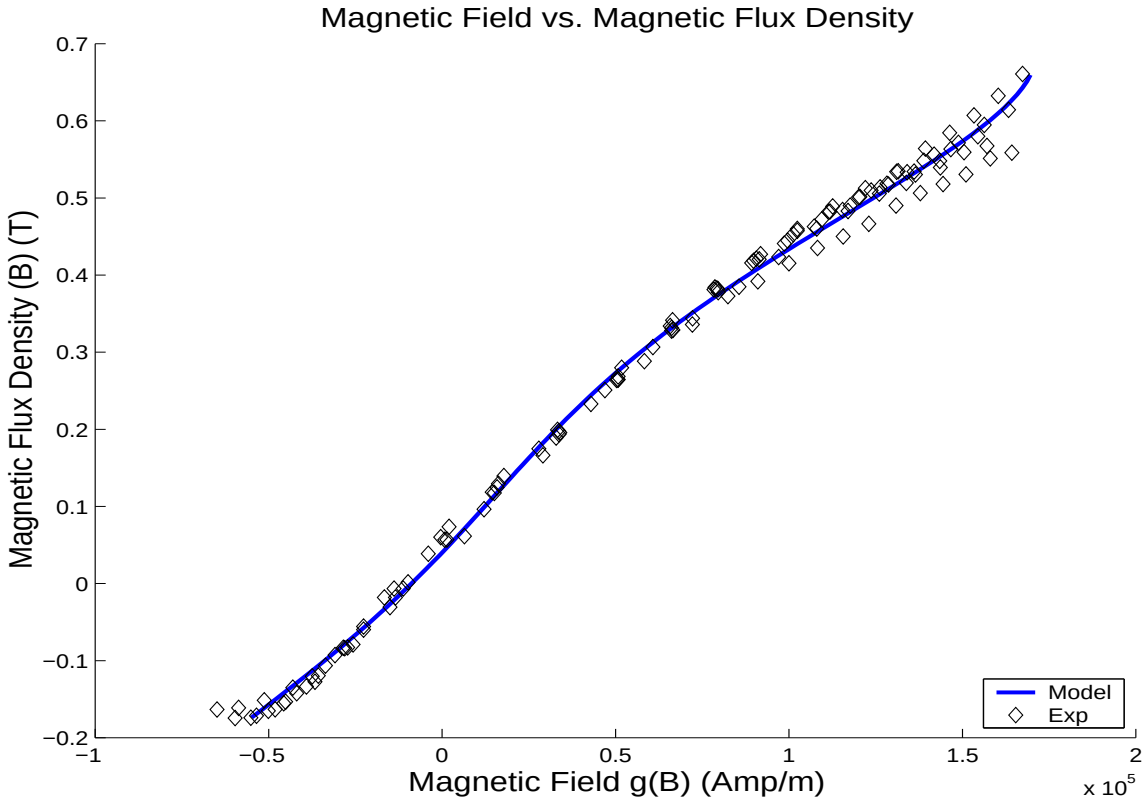

(b)

Figure 2.23: Nonlinear curves (a) Strain vs. Stress curve (b) Magnetic field vs. Magnetic flux density curve.

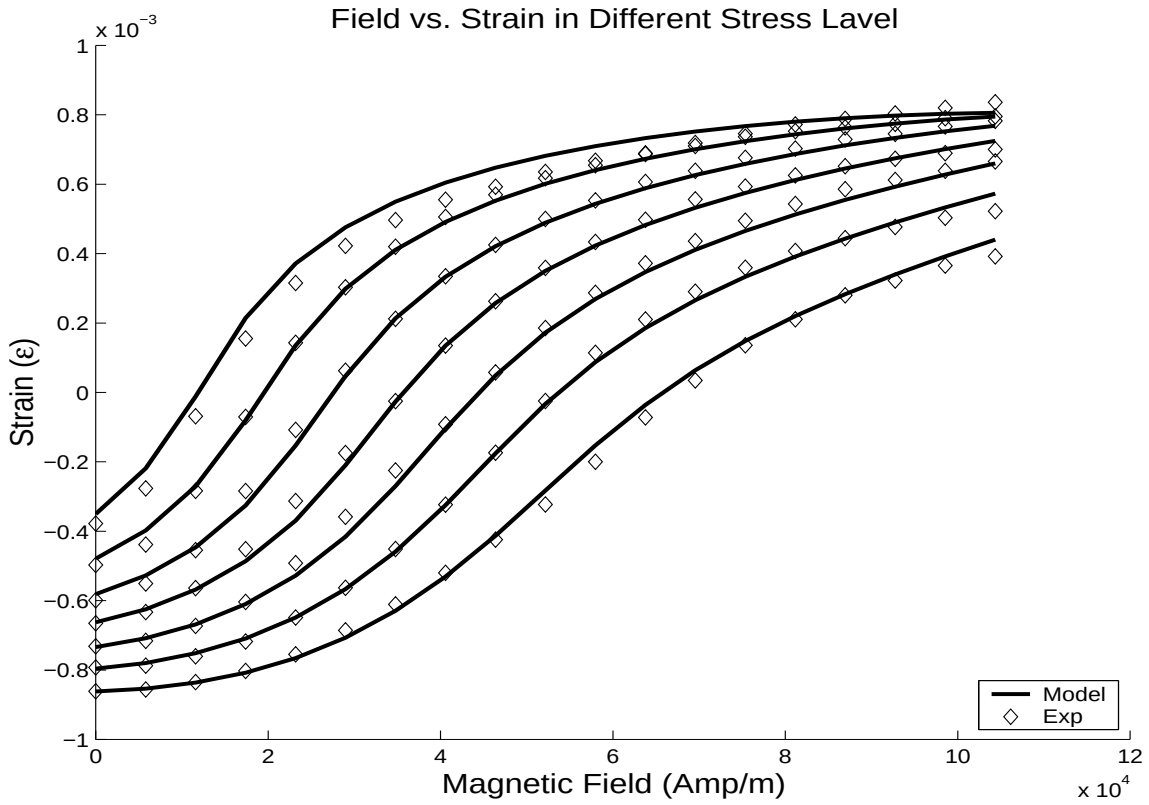

(a)

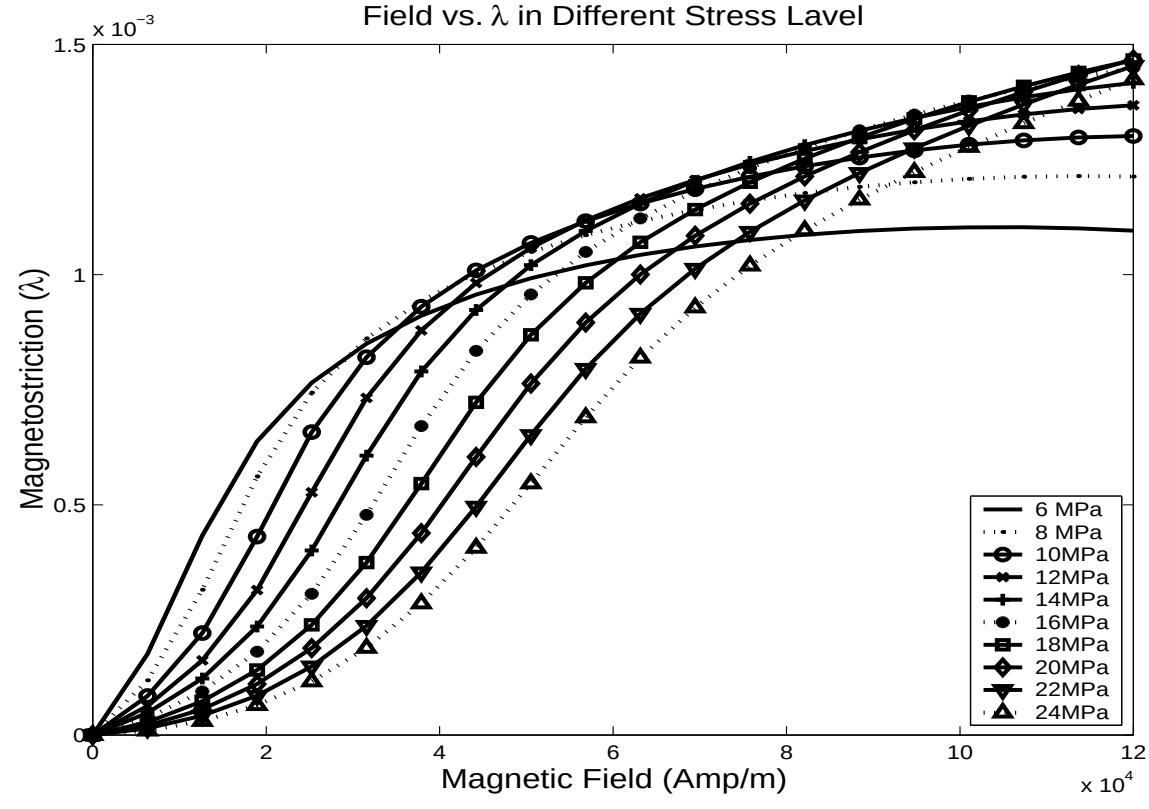

(b)

Figure 2.24: Nonlinear curves in different stress level (a) Magnetic field vs. Strain (b) Magnetic field vs. Magnetostriction.

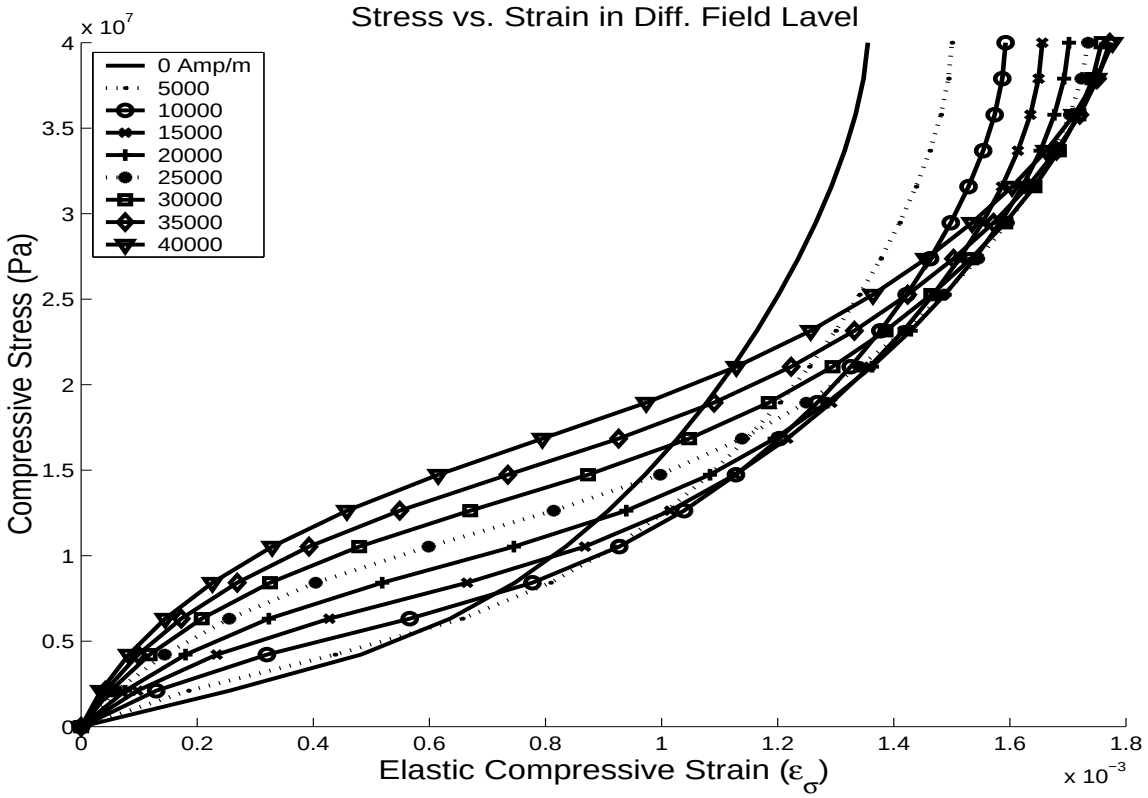

(a)

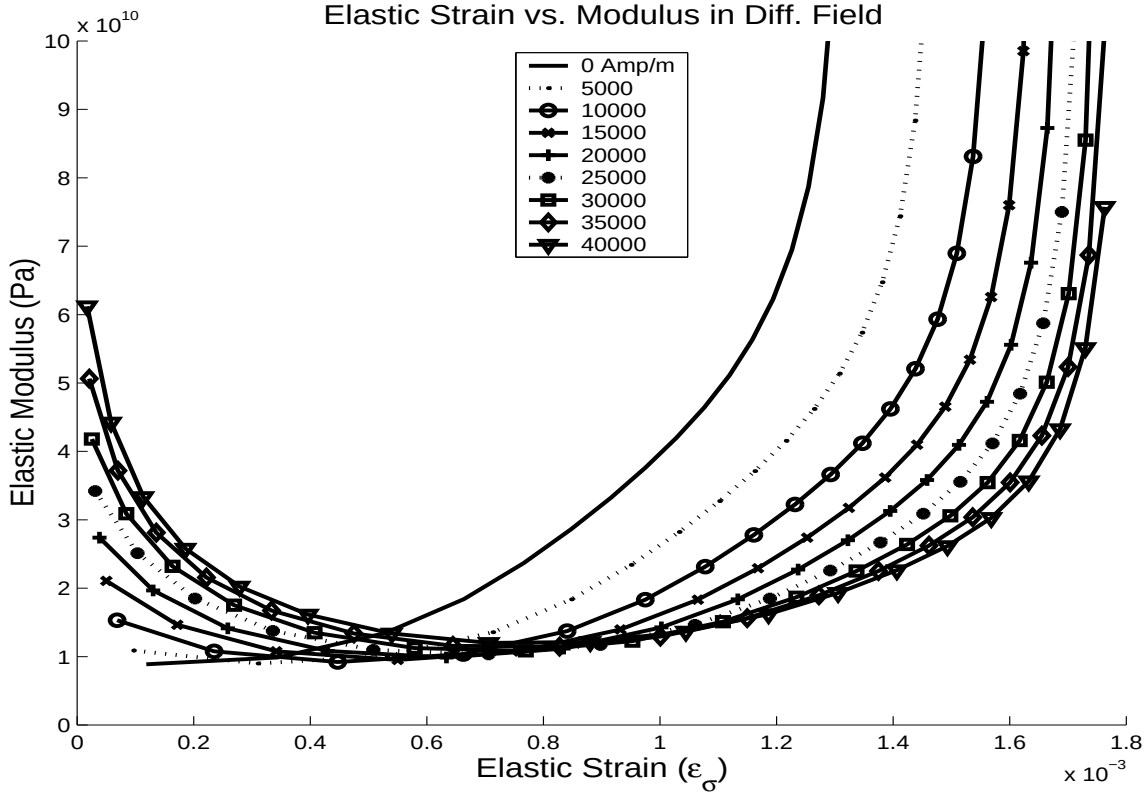

(b)

Figure 2.25: Nonlinear curves for different field level (a) Stress vs. Strain (b) Modulus vs. Strain.

Equation-(2.43) the value of strain is evaluated considering magnetic field as coil current times coil turn per unit length of actuator. Using this strain, from the $\epsilon - E(\epsilon)$ curve the value of $E(\epsilon)$ can be found. From Equation-(2.42), the value of B can be determined. If this B value is not same as assumed, this iteration will be continued until the value converges.

2.3.3 ANN Model.

To avoid iterative procedure mentioned in the nonlinear model, one three layer artificial neural network is developed, which gives direct nonlinear mapping from the magnetic field and the stress to the magnetic flux density and the strain (Figure-2.26). Standard logistic function $y = 1/(1+e^{-1.7159v})$ is used in the hidden layer as activation function with linear output layer. The input (stress and magnetic field) and the output (strain and magnetic flux density) data are normalized for better performance of network.

$$\sigma_n = \frac{(\sigma - \sigma_{mean})}{(max|\sigma| - \sigma_{mean})} \tag{2.54}$$

$$H_n = \frac{(H - H_{mean})}{(max|H| - H_{mean})} \tag{2.55}$$

$$\epsilon_n = \frac{(\epsilon - \epsilon_{mean})}{(max|\epsilon| - \epsilon_{mean})} \tag{2.56}$$

$$B_n = \frac{(B - B_{mean})}{(max|B| - B_{mean})} \tag{2.57}$$

σ_n, the normalized stress is calculated using Equation-(2.54). The value of σ_{mean} and $(max|\sigma| - \sigma_{mean})$ are $-1.57966X10^7$ and $0.830345X10^8$ Pa respectively. Similarly H_n is normalized magnetic field, is calculated from Equation-(2.55). The value of H_{mean} and $(max|H| - H_{mean})$ in Equation-(2.55) are both 750 Oe. Normalized strain ϵ_n is the output of network, from which strain is calculated using Equation-(2.56). The value of ϵ_{mean} and $(max|\epsilon| - \epsilon_{mean})$ are $0.203245X10^{-03}$ and $0.106504X10^{-02}$ respectively. In Equation-(2.57) the value of B_{mean} is 0.385126 tesla and the value of $(max|B| - B_{mean})$ are 0.319818 and 0.499656 tesla respectively. To train this network, some training and validation samples are generated through iterative process stated earlier. Weight and bias parameter of the trained network is given in Table-2.5 and Table-2.6, respectively. Different validation studies are also carried out.

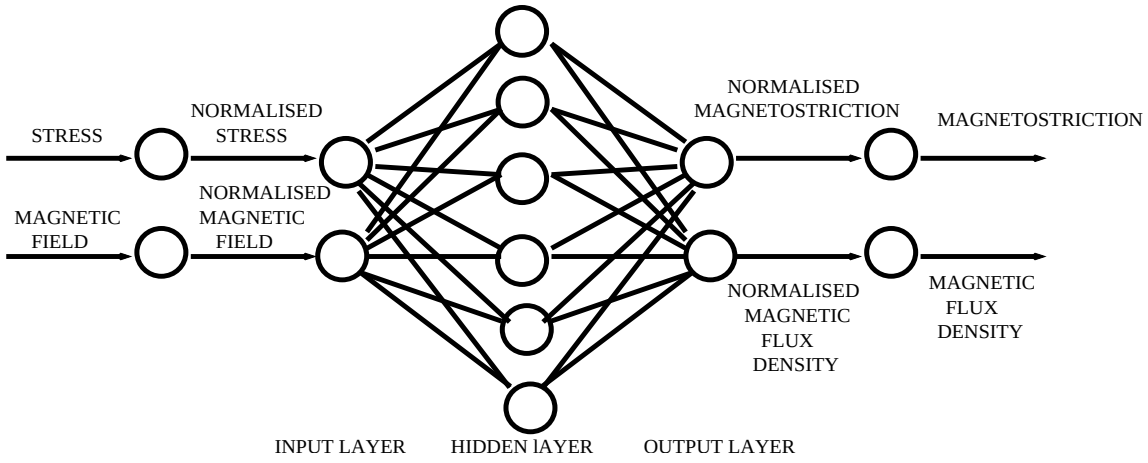

Figure 2.26: Artificial neural network architecture

Table 2.5: Connection between input layer and hidden layer.

Input Layer Neurons	Hidden Node 1	Hidden Node 2	Hidden Node 3	Hidden Node 4
H_n	4.6187	-2.1241	-.15066	.38726
σ_n	1.2866	-1.3195	-.43318	.031765
Input Bias	2.2483	-.25721	-.61579	.088719

2.3.4 Comparison between Different Coupled Models.

Comparative studies of different models are done taking a magnetostrictive rod with varying magnetic field and stress level. Three different stress levels (6.9 MPa,15.1 MPa and 24.1MPa) are taken to compute the total strain and magnetic flux density in the rod for varying magnetic field level and shown in Figure-2.27. In Figure-2.27(a), total strain is shown according to linear, polynomial, ANN and experimental approaches. Both polynomial and ANN approach is showing close result with the experimental data throughout the magnetic field range. Where as in linear model, results are not matching with the experimental data throughout the magnetic field range. But, this model can be used in low magnetic field level for medium stress level and in medium field level for high stress level. For low stress level, linear model can be used in an average sense. In the absence of experimental data (Etrema manual) of magnetic flux density, only computational results are shown in Figure-2.27(b). Magnetic flux density is shown according to linear, polyno-

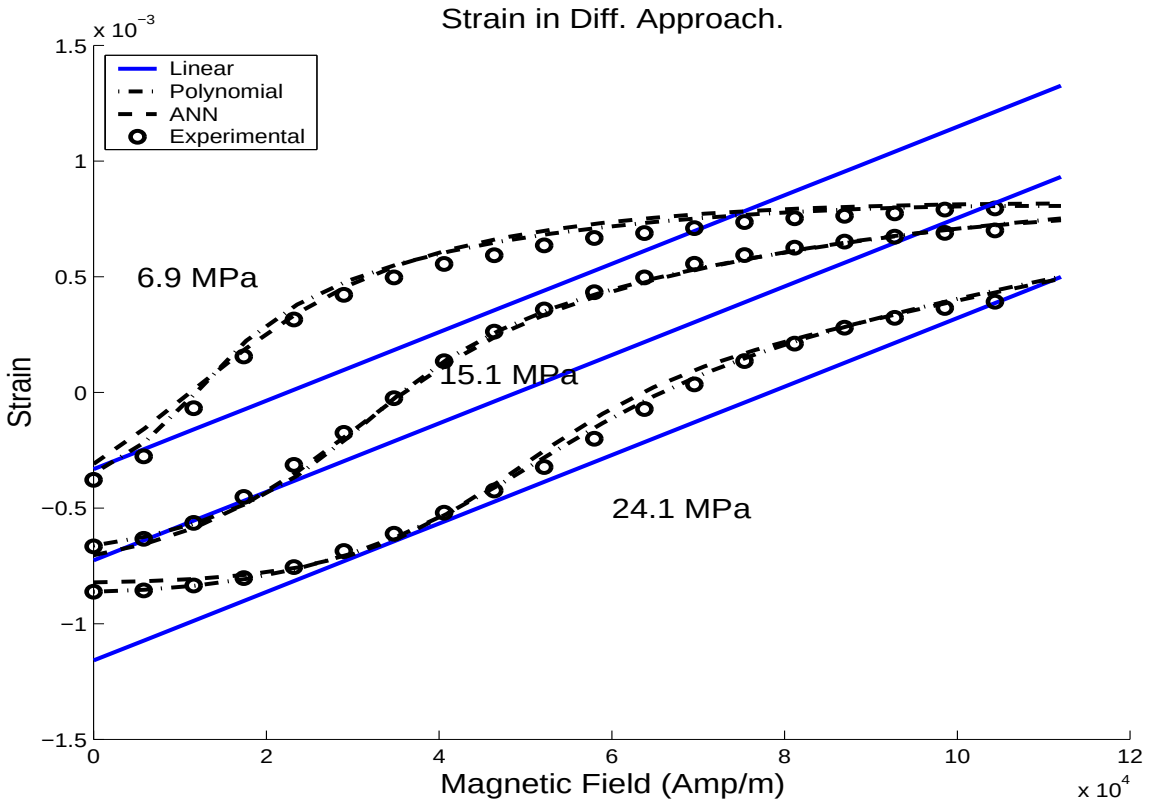

(a)

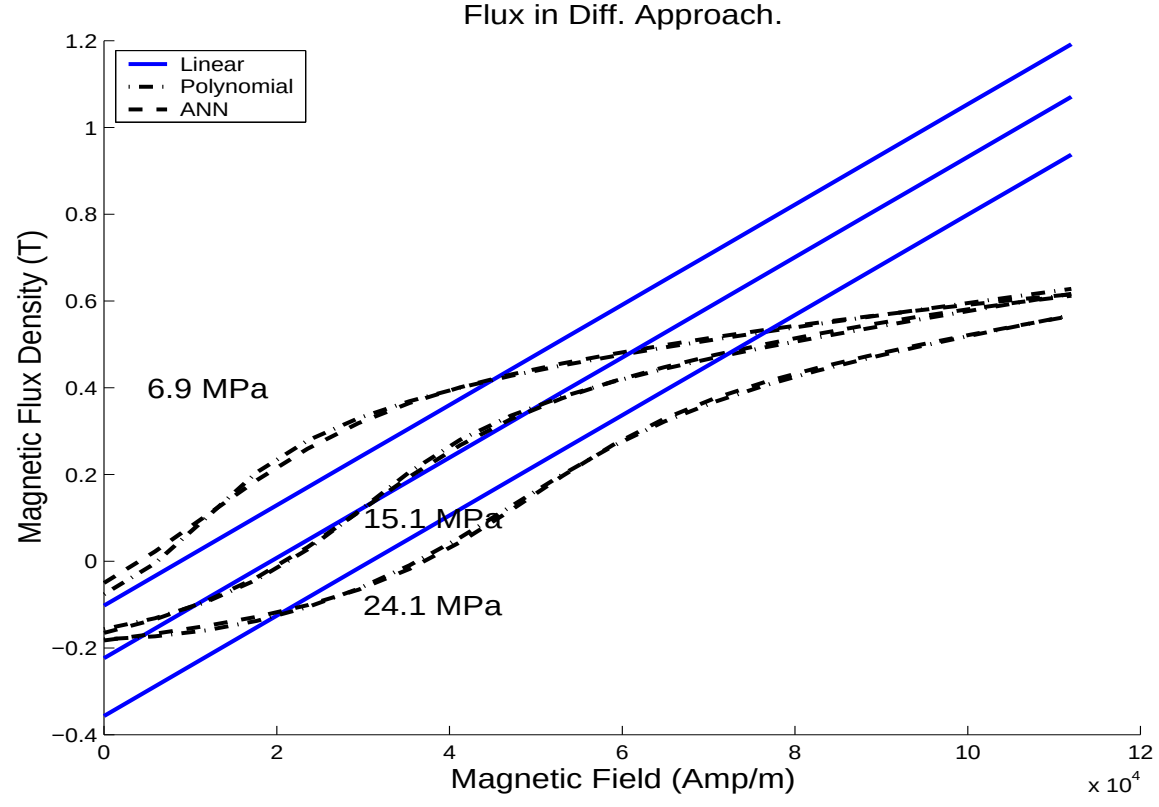

(b)

Figure 2.27: Nonlinear curves for different stress level (a) Strain vs. Magnetic field (b) Magnetic flux density vs. Magnetic field.

Table 2.6: Connection between hidden layer and output layer.

Output Layer Neurons	ϵ_n	B_n
Hidden Node 1	.63447	.67409
Hidden Node 2	-.53313	-.23172
Hidden Node 3	-.69546	-.071654
Hidden Node 4	.48235	2.1900
Output Bias Node	-.29930	-1.5467

mial and ANN approach. Similar to strain result, results of ANN model and polynomial model are in excellent agreement. However, the results of linear model are not matching through out the magnetic field range. In the linear model, for medium stress level, the magnetic flux density is matching with the nonlinear model. For high and low stress level, linear model can be used in an average sense.

2.4 Summary

This study is mainly intended for anhysteretic linear, nonlinear, uncoupled and coupled constitutive relationship of magnetostrictive material. Nonlinearity in these relationships is studied using polynomial representation and artificial neural network (ANN).

In uncoupled model, sensor and actuator equations are separately studied assuming that the magnetic field as strain independent. In linear-uncoupled model, modulus of elasticity, permeability and magnetomechanical coupling coefficient are considered as constant. In nonlinear–uncoupled model, magnetostriction is represented through a three layer artificial neural network for actuation property, which is trained and validated from Etrema manual.

Coupled model is studied without assuming any direct relationship of magnetic field. In linear-coupled model, elastic modulus, permeability and magnetoelastic constant is assumed as constant. But this model cannot predict the highly nonlinear properties of magnetostrictive material. In nonlinear-coupled model, nonlinearity is decoupled in magnetic domain and mechanical domain using two nonlinear curves for stress-strain and magnetic flux density-magnetic field intensity. In this model, the computation of magnetostriction requires the value of magnetic flux density, which comes through an iterative process for nonlinearity of curves. To avoid this iterative computation, one three layer artificial neural network is developed, which will give nonlinear mapping from the stress level and the magnetic field to the strain and the magnetic flux density. Finally,

comparative study of linear, polynomial and ANN approach is performed and shown that linear coupled model can predict the constitutive relationships in an averaged sense only. Nonlinear models are shown to predict experimental results exactly throughout the magnetic field range.

In the next and the subsequent chapter, we will use these material models in the finite element model and qualitatively show the differences in the responses predicted by these models. It will also be shown how these models will have an impact on the SHM studies.